Methods Of Generating Body Designs For Vehicles Such As Ships

Technical Field

The present invention relates to the optimisation of transportation / vehicular body designs, in particular hull designs for a ship, using a morphing evolutionary approach in the design and manufacture process.

Background

With more stringent environmental regulations to reduce carbon footprint, eco-friendliness and high energy efficiency are now key criteria for the design and construction of all new ships. Hull Form Design and Optimisation (HFDO) is an integral part of the ship design process where the hull shape is modelled, modified and evaluated in an iterative manner to improve the overall design. An efficient hull form will help to reduce the overall drag acting on the ship and reduce fuel consumption and harmful emission to the environment.

Traditional method of ship design and hull form optimisation requires many hours by the designer using a 'trial-and-error' approach, which is inefficient and does not guarantee optimum designs. More recently, simulation-based design (SBD) methods have been adopted to improve the efficiency of the hull form design. However, the design process still requires considerable human input and success at the end depends very much on the designer's experience and knowledge. In addition, existing geometry modification methods also depend on the designer to provide the parameters for shape variations and hence may limit the creation of more diverse hull forms. Some existing methods require additional pre-check steps such as design-of-experiment (DOE) to ensure that variations defined by the designer helps to reasonably improve the design with no unfeasible designs. DOE is often used as a preliminary exploration of the design space to investigate the influence of parameters on the objectives and to provide a first idea of the expected performance and as to which parameters have the most impact on the overall design optimisation process. While computational fluid dynamic (CFD) analysis becomes more accurate and is increasingly used for evaluating the performance of hull form design, they are highly computationally expensive and not suitable for evaluating large number of designs, in particular at an early stage of the design and manufacturing process.

Thus, there is a need for a more efficient method to generate new and diverse solutions, preferably with minimal user input.

Summary of Invention

In a first aspect there is provided a computer implemented method of generating a new body design for a new vehicle, the method comprises:

(a) providing an initial body design of a vehicle in a two-dimensional space with a plurality of frame lines;

(b) selecting a first boundary frame line of the initial body design and a second boundary frame line of the initial body design;

(c) selecting a first reference frame line between the first boundary frame line and the second boundary frame line;

(d) selecting a morphing parameter, wherein the morphing parameter is a rate of change between the first reference frame line and the first boundary frame line and/or the second boundary frame line;

(e) modifying the initial body design from the first reference frame line towards the first boundary frame line and/or from the first reference frame line towards the second boundary frame line based on the morphing parameter; and

(f) generating the new body design.

Preferably, there is at least one intermediate frame line between the first reference frame line and the first boundary frame line and/or the first reference frame line and the second boundary frame line, and the method further comprises adjusting the at least one intermediate frame line based on a modified morphing parameter. In an example, the reference frame line is modified based on the morphing parameter while the intermediate frame line/s is/are adjusted by the modified morphing parameter. The modified morphing parameter for the intermediate frame line/s have an intermediate value between the morphing parameter at the reference frame line and the boundary frame line. The modified morphing parameter may gradually increase or decrease from the value of the morphing parameter of the reference frame line as it moves away from the reference frame line. The modified morphing parameter is thus dependent on the value of the morphing parameter and the position of the intermediate frame line from the reference frame line. As an example, the modified morphing parameter may increase or decrease in a linear or non-linear manner. Advantageously, this allows the body design to remain smooth.

Preferably, the method further comprises selecting a third boundary frame line of the initial body design; selecting a second reference frame line between the second boundary frame line and the third boundary frame line; selecting a second morphing parameter, wherein the

second morphing parameter is a rate of change between the second reference frame line and the second boundary frame line and/or the third boundary frame line and modifying the initial body design from the second reference frame line towards the second boundary frame line and/or towards the third boundary frame line based on the second morphing parameter.

Preferably, the first, second, and/or third boundary frame lines is/are a non-terminal frame line. Advantageously, this minimises or avoids unfeasible body designs at the extreme ends of the body design.

Preferably, the first boundary frame line is selected proximal to a first end of the initial body design and the second boundary frame line is selected proximal to a second end of the initial body design, the second end being opposite to the first end. For example, the first end may be the forward or bow section of a ship, and the second end is the aft or stern section of the ship. The region between the first and second boundary frame lines may form a substantial portion of the body design. For example, the region between the two frame lines may be at least 50% of the body design, at least 60% of the body design, at least 70% of the body design, or at least 80% of the body design or at least 90% of the body design or at least 95% of the body design. For example, the region between the two frame lines may be at most 95% of the body design, or at most 90% of the body design. For example, the region between the two frame lines may be 50% to 95% of the body design, or 60% to 95% of the body design, or 70% to 95% of the body design, or 80% to 95% of the body design, or 90% to 95% of the body design. Alternatively, the region between the two frame lines may be 50% to 90% of the body design, or 60% to 90% of the body design, or 70% to 90% of the body design, or 80% to 90% of the body design. This allows a substantial portion of the body design to be effectively modified in a simple and efficient manner while avoiding the extreme ends of the body designs. The first, second, and third (if present) boundary frame lines are preferably selected by the user based, or predefined.

In an example, the first boundary frame line is selected from the forward section of the body design, the second boundary frame line is selected from the aft section of the body design, and the reference frame line is in between the two boundary frame lines. Proximal includes being both near and at the point of reference.

Preferably, the first end is a forward section of the initial body design, the second end is an aft section of the body design, and the third boundary frame is selected proximal to the middle of the initial body design. In an example, the first boundary frame line is selected from the forward section of the body design, the second boundary frame line is selected from the aft section of the body design, and a third boundary frame line is selected proximal to the middle of the initial body design. The three boundary frame lines may preferably divide the body design into a forward body and an aft body. The first reference frame line may be selected from the forward body (between the first and third boundary frame lines) and the second reference frame line may be selected from the aft body (between the second and third boundary frame lines). Advantageously, this allows the forward section and aft section to be modified differently and according to different considerations as most if not all vehicles (such as ships, cars, and aeroplanes) have distinct differences in their forward and aft body due to hydrodynamic and/or aerodynamic considerations.

Preferably, the morphing parameter is randomly selected. More preferably, the morphing parameter is randomly selected within defined constraints. Advantageously, this allows the generation of diverse solutions without a user's bias.

Preferably, the first reference frame line and/or the second reference random frame line are randomly selected. Advantageously, this allows for random modification of the body design and allows for the creation of unique and diverse solutions.

Preferably, modifying the initial body design is based on the following:

$Y(t = x_R \times W\ )_{R_{x,z}} = (1 - (t \times S_{TS})) \times Y_{S_{x,z}} + (t \times S_{TS}) \times Y_{T_{x,z}}$,

where $W = 0.02 \times (x - x_{AB})$ when $x_{AB} \leq x \leq x_{MB}$ and$W = 0.02 \times (x - x_{MB})$ when $x_{MB} \leq x \leq x_{FB}$;

$Y(t = x_A\ \times W)_{A_{x,z}} = (1 - (t \times S_{TS})) \times Y_{S_{x,z}} + (t \times S_{TS}) \times Y_{T_{x,z}}$,

where $W = 0.04 \times (x - x_R)$ when $x_R \leq x \leq x_{MB}$ and $x_R \leq x \leq x_{FB}$,

$W = 0.04 \times (x_R - x)$ when $x_{AB} \leq x \leq x_R$, and

$W = 0.04 \times (x - x_{MB})$ when $x_{MB} \leq x \leq x_R$;

subject to $0.2 \leq t \leq 0.8$ and smoothing factor, $S_{TS} = 1 - \frac{Y_{TS}}{B_{max}}$,

where $Y(t)_{R_{x,z}}$ is the new *Y* value for the reference curve at corresponding *x* and *z* coordinates, $Y(t)_{A_{x,z}}$ is the new *Y* value for adjacent curves at corresponding *x* and *z* coordinates, $Y_{S_{x,z}}$ is the *Y* value for the reference (source) curve at corresponding *x* and *z*

coordinates and $Y_{T_{x,z}}$ is the Y value for the boundary (target) curve at corresponding x and z coordinates. x_A is the x coordinate of the adjacent frame between the reference frame and boundary frames, $x_{F/AB}$ is x frame at the forward or aft boundary section, x_R is x frame at the reference frame section and x_{MB} is x frame at the mid boundary section. W is the weightage, Y_{TS} is the Y value of the transition section between the two boundaries and B_{max} is the maximum ½ breadth.

Preferably, the vehicle is a ship. In other words, the body design is a hull design.

Preferably, providing the initial body design in a two-dimensional space with a plurality of frame lines comprises providing dimensions of the initial body design in a two dimensional offset table and mapping the dimensions in the two dimensional offset table into a two dimensional line plan to obtain the plurality of frame lines. The two dimensional line plan may be viewed the superimposition of multiple cross sections on to a plane. Advantageously, this allows for a simple and direct conversion of the body design while allowing for efficient modification of the body design.

In a second aspect there is provided a computer implemented method of generating a new set of body designs for a new vehicle, the method comprises:

(a) providing a set of body designs of a vehicle;
(b) evaluating each body design in the set with respect to at least one objective function;
(c) performing a crossover combination of a plurality of body designs from the set to provide a plurality of initial body designs based on a crossover rate, wherein the crossover rate is a probability of the combination occurring;
(d) providing each of the plurality of initial body designs in a two-dimensional space with a plurality of frame lines;
(e) selecting a first boundary frame line of each of the initial body designs and a second boundary frame line of each of the initial body designs;
(f) selecting a first reference frame line between the first boundary frame line and the second boundary frame line;
(g) selecting a morphing parameter, wherein the morphing parameter is a rate of change between the first reference frame line and the first boundary frame line and/or the second boundary frame line;

(h) modifying each of the initial body designs from the first reference frame line towards the first boundary frame line and/or from the first reference frame line towards the second boundary frame line based on the morphing parameter and a mutation rate, wherein the mutation rate is a probability of modifying the initial body design;

(i) generating a plurality of new body designs;

(j) evaluating the plurality of new body designs based on the at least one objection function;

(k) ranking the body designs in the set of body designs and in the plurality of new body designs based on the evaluation of the at least one objective function; and

(l) generating a new set of body designs based on the ranking.

Preferably, embodiments of the first aspect apply to the second aspect.

Preferably, the method further comprises selecting the plurality of body designs randomly from the set to perform the crossover combination or selecting the plurality of body designs based on the evaluating step to perform the crossover combination.

Preferably, the method further comprises rescaling at least one of the body designs in the selected plurality of body designs prior to performing the crossover combination.

Preferably, ranking the body designs comprises sorting the body designs in the set of body designs and the plurality of new body designs to determine at least one Pareto front; measuring a distance between each body design in each of the at least one Pareto front; and ordering the body designs in the set of body designs and the plurality of new body designs based on the at least one Pareto front and the distance between the body designs in each Pareto front.

Preferably, the method comprises repeating steps (c) to (l) using the new set of body designs until convergence of the body designs or a maximum number of iterations is reached.

Preferably, the at least one objective function is any one selected from the group consisting of manoeuvrability, resistance, seakeeping, stability, and structural strength.

Preferably, the set of body designs comprises a plurality of existing body designs. More preferably, the set of body designs comprises at least one modified body design obtained by interpolating and/or extrapolating a first existing body design and a second existing body design. This may be particularly useful when the initial set of body designs is small and may contain insufficient body designs resulting in sub-optimisation or a reduced solution space.

Preferably, each of the first existing body design and the second existing body design is represented in a two dimensional plane at a plurality of locations along a third dimension perpendicular to the two dimensional plane.

Preferably, the crossover rate and/or mutation rate is at least 0.5, more preferably wherein the crossover rate and/or mutation rate is at least 0.7 (i.e. from 0.7 to 1 inclusive of both end points). Advantageously, this is independent on the initial body design/s used thus allowing for a process requiring minimal to negligible user input, experience, or bias.

Preferably, the new set of body designs has the same number of body designs as the set of (existing) body designs. Preferably, the number of new body designs generated is the same as the number in the set of body designs.

In a third aspect, there is provided a method to build a vehicle, the method comprises obtaining the new body design for a vehicle according to the first aspect or obtaining the new set of body designs for a vehicle according to the second aspect, and manufacturing the vehicle based on the new body design or the new set of body designs.

In a fourth aspect, there is provided a non-transitory computer readable medium comprising instructions which, when executed by a computer, cause the computer to perform a method according to the first aspect or the second aspect.

Brief Description of Figures

In the Figures:

Figure 1 shows an embodiment of a method to obtain a new body design;

Figure 2 shows an example of an offset table of a vessel with width (half-breadth), length (frames), and height (waterlines) values in metres;

Figure 3 shows a hull form represented in the form on an offset table, 2D lines plan and 3D model;

Figure 4 shows 2D curve morphing through interpolation and extrapolation on vessel A (source) and vessel B (target);

Figure 5 shows curve correspondence using cubic spline interpolation;

Figure 6 shows two existing vessels (ship 1 and ship 2) and its corresponding station number and morphing parameters *t*;

Figure 7 shows a wire mesh diagram of two parent vessels and intermediate vessels created by constant-morph using different morphing parameter (*t*);

Figure 8 shows a combination of ship A aft body and ship B forward body;

Figure 9 shows a crossover between ship A aft and ship B forward body through cross-morph concept;

Figure 10 shows morphing through cross-morph applied to mid body of combined ship A (aft) and ship B (forward);

Figure 11 shows morphing through cross-morph applied to a combined vessel A (aft) and vessel B (forward), Figure 11(a) show cross-morph applied nearer to forward of ship B and retained aft of ship A and Figure 11(b) shows cross-morph applied nearer to aft of ship A and retained forward of ship B;

Figure 12 shows an example of how cross morph may be applied by combining ship A aft section, ship B mid-section and ship C forward section.

Figure 13(a) shows a sample vessel C body plan and Figure 13(b) shows a combination of vessel A aft body, vessel B mid body and vessel C forward body

Figure 14 shows a wire mesh diagram of two parent vessels (Pipe-lay and VLCC);

Figure 15 shows a combination of pipe-lay forward body and VLCC aft body without cross-morph;

Figure 16(a) shows a wire mesh diagram and Figure 16(b) shows the 3D surfaces of a combined vessel from pipe laying vessel A and VLCC vessel B with cross-morph;

Figure 17 shows a two-point cross-morph of Ship A aft, ship B mid, and ship C forward body;

Figure 18 shows a combination of three different vessel types using cross-morph;

Figure 19 shows a mix-and-match of different designs using cross-morph approach;

Figure 20 shows a boundary-morph concept for aft (A) and forward section (B)

Figure 21 shows a wire mesh diagram of an original hull form of container vessel A with boundary frames set at station 10 (forward), station 5 (midship) and station 0 (aft);

Figure 22 shows wire mesh diagrams of a modified hull form using boundary-morph (a) inward shifting from forward reference curve (station 7.5) to forward boundary curve (station 10), (b) inward shifting from aft reference curve (station 2.5) to aft boundary curve (station 0), (c) outward shifting from forward reference curve (station 7.5) to mid boundary curve

(station 5), (d) outward shifting from aft reference curve (station 2.5) to mid boundary curve (station 5);

Figure 23 shows the concepts of encoding where a solution (phenotype) is mapped into a chromosome (genotype) and decoding where a chromosome is converted back into its corresponding actual solution;

Figure 24 shows the working principles of genetic algorithm (GA);

Figure 25 shows the working principle of NSGA-II featuring non-dominated sorting and crowding distance;

Figure 26 shows a morphing evolutionary approach;

Figure 27 shows a schematic diagram of an embodiment;

Figure 28 shows an embodiment of a method to obtain a new set of body designs;

Figure 29 shows feasible and infeasible solution with constraint boundaries;

Figure 30 shows changing of section shape based on a linear proportions approach;

Figure 31 shows phenotype-genotype mapping using real value chromosome (initial value of t = 0);

Figure 32 shows the pseudo code for replacement using distance crowding method from NSGA-II;

Figure 33(a) shows an example of a solution space of GA without elitism;

Figure 33(b) shows an example of a solution space of NSGA-II with elitism;

Figure 34 shows the convergence plot with a crossover rate of 0.1 to 1.0 and mutation rate of 0 to evaluate the effects of the crossover only;

Figure 35 shows the convergence plot (right) with a mutation rate of 0.1 to 1.0 and crossover rate of 0 to evaluate the effects of mutation only;

Figures 36A and 36B shows wire mesh diagrams of existing (parent) ships;

Figures 37A and 37B shows body plans of existing (parent) ships;

Figure 38 shows the wire-mesh diagrams of initial parents and child vessels from generation 1 of the optimisation;

Figures 39(a)-(f) shows the convergence plot with different crossover rates and mutation rates;

Figure 40 shows a solution space for a crossover rate of 0.8 and mutation rate of 0.7;

Figure 41 shows the wire-mesh diagrams of the child vessels from generation 1 of the optimisation;

Figure 42 shows a body plan comparing the best child (solution 1189) and the best initial parent (Ship 1 – Container Ship A);

Figures 43(a)-(f) shows the convergence chart with different crossover rates and mutation rates;

Figure 44 shows the convergence chart with different crossover rates and without mutation;
Figure 45 shows a solution space for a crossover rate of 0.7 and mutation rate of 1.0;
Figure 46 shows the body plan comparing the best child (Solution 397) and the best initial parent (Ship 1 – Container Ship A);
Figure 47 shows the wire-mesh diagrams of the hull form for child solutions at different generations;
Figure 48 shows the initial hull form expansion with 8 new child vessels created from 4 initial parents through constant-morph;
Figures 49(a)-(f) shows the convergence chart with different crossover rates and mutation rates;
Figure 50 shows a solution for a crossover rate of 1.0 and mutation rate of 0,8, in which "Initial'" represents the initial population's solutions generated through constant-morph;
Figure 51 shows the body plan comparing the best child (Solution 1189) and the best initial parent (Ship no. 1 – Container Ship A);
Figure 52 shows the wire-mesh diagrams of child solutions at different generations;
Figure 53 shows the 3D surface of a container vessel created in NAPA;
Figure 54 shows the FFD transformation comparing initial (dotted) and transformed hull (bolded);
Figure 55 shows a panelised surface using 1960 hull panels and 1000 free surface panels;
Figure 56 shows a wave profile of an optimised design (solution ID 96);
Figure 57 shows a two-point cross-morph combining ship 9 (VLCC), ship 1 (container A) and ship 7 (product tanker);
Figures 58(a)-(f) shows the convergence charts for total resistance with crossover rates of (a) 0.5, (b) 0.6, (c) 0.7, (d) 0.8, (e) 0.9, (f) 1.0 and mutation rates ranging from 0.5 to 1;
Figure 59 shows the convergence charts for heave showing crossover rates of (a) 0.5, (b) 0.6, (c) 0.7, (d) 0.8, (e) 0.9, (f) 1.0 and mutation rates ranging from 0.5 to 1.0;
Figure 60 shows a convergence chart of resistance and heave;
Figure 61 shows a solution space showing the performance of the initial parents and child solutions for optimising resistance and heave motion;
Figure 62 shows the wire-mesh diagrams of the best child (a) solution 1190 and (b) solution 1194;
Figure 63 shows the body plans comparing (a) best child solution 1190 with best initial parent – ship 11 for heave, and (b) best child solution 1194 with best initial parent – ship 1 for resistance;
Figure 64 shows the convergence charts of total resistance with crossover rates of (a) 0.5, (b) 0.6, (c) 0.7, (d) 0.8, (e) 0.9, (f) 1.0 and respective mutation rates ranging from 0.5 to 1;

Figure 65 shows the convergence charts of heave with crossover rates of (a) 0.5, (b) 0.6, (c) 0.7, (d) 0.8, (e) 0.9, (f) 1.0 and respective mutation rates ranging from 0.5 to 1;
Figure 66 shows the convergence charts of pitch with crossover rates of (a) 0.5, (b) 0.6, (c) 0.7, (d) 0.8, (e) 0.9, (f) 1.0 and respective mutation rates ranging from 0.5 to 1;
Figure 67 shows the convergence charts of roll with crossover rates of (a) 0.5, (b) 0.6, (c) 0.7, (d) 0.8, (e) 0.9, (f) 1.0 and respective mutation rates ranging from 0.5 to 1;
Figure 68 shows the combined convergence chart for resistance, heave, pitch and roll;
Figure 69 shows the solution space for heave and resistance;
Figure 70 shows the solution space for pitch and resistance;
Figure 71 shows the solution space for roll and resistance;
Figure 72 shows the solution space for heave and pitch;
Figure 73 shows the solution space for heave and roll;
Figure 74 shows the solution space for roll and pitch;
Figure 75 shows the best initial parent and child solutions for optimising four objective functions;
Figure 76 shows the wire-mesh diagrams of the best child for (a) heave (solution 1190), (b) resistance (solution 1192), (c) pitch (solution 1191), and (d) roll (solution 1193);
Figure 77 shows the body plans comparing (a) the best child (solution 1190) and the best initial parent (ship 11) for heave, (b) the best child (solution 1192) and the best initial parent (ship 1) for resistance, (c) the best child (solution 1191) and the best initial parent (ship 10) for pitch and (d) the best child (solution 1193) and the best initial parent (ship 7) for roll;
Figure 78 shows the solution space with a goal setting approach for a) resistance and heave, b) resistance and pitch, c) resistance and roll, d) pitch and heave, e) pitch and roll and f) roll and heave (the constraint limits for each objective are shown in the dashed lines).

Detailed Description

Features that are described in the context of an embodiment may correspondingly be applicable to the same or similar features in the other embodiments. Features that are described in the context of an embodiment may correspondingly be applicable to the other embodiments, even if not explicitly described in these other embodiments. Furthermore, additions and/or combinations and/or alternatives as described for a feature in the context of an embodiment may correspondingly be applicable to the same or similar feature in the other embodiments.

Modifications, additions, or omissions may be made to the systems, apparatuses, and methods described herein without departing from the scope of the disclosure. For example,

the components of the systems and apparatuses may be integrated or separated. Moreover, the operations of the systems and apparatuses disclosed herein may be performed by more, fewer, or other components and the methods described may include more, fewer, or other steps. Additionally, steps may be performed in any suitable order. As used in this document, “each” refers to each member of a set or each member of a subset of a set.

As used herein, the articles “a”, “an” and “the” as used with regard to a feature or element include a reference to one or more of the features or elements. As used herein, the term “and/or” includes any and all combinations of one or more of the associated listed items. As used herein, the terms “first,” “second,” and “third,” etc. are used merely as labels, and are not intended to impose numerical requirements on their objects.

As user herein, “x, y, z” coordinates and/or axis may be used to illustrate dimensional axes without being limited in any specific direction.

The term “aft” refers to the rear of a ship or moving towards the rear of the ship. The term “stern” may refer to the back of the ship or the rear most part of the ship. The term “forward” (“fwd”) or “fore” refers to the front of the ship or moving towards the front of the ship. The term “bow” may refer to the forward part of the ship or the most forward part of the ship.

Metamorphosis, also known as morphing, is the sequential construction of intermediate objects that represent the gradual transition from one object to another. Since the beginning of shipbuilding and introduction of computer-aided design (CAD), a two-dimensional (2D) offset table remains the most fundamental representation of ship’s hull form, and is still used as the basis for designer to model and modify the hull design. An offset table comprises key information of the hull geometry - length, breath and height values- which are represented in terms of half breath of waterlines, height of buttocks, flat of bottom and flat of side. A key advantage of using a 2D curve by linking up the coordinate points from offset table is the simplicity to represent the entire shape of the hull and ease to modify the hull form by adjusting the lines. A 2D representation is unlikely to represent the entire hull form as accurately as a three-dimensional (3D) representation but this inaccuracy is considered negligible if the 2D representation is used as a reference during initial design stage. A sample offset table of a vessel consisting of width (half-breath) values with respect to length (frames) position and height (waterlines) are shown in Figure 2.

An existing (or initial) body design may be provided in a two-dimensional space with a plurality of frame lines by providing dimensions of the initial body design in a two dimensional offset table and mapping the dimensions in the two dimensional offset table into a two dimensional line plan to obtain the plurality of frame lines.

These 2D offset data can be mapped into a 2D lines plan comprising a body plan, a half-breath plan and a sheer plan. Thus, each of the body plan, half-breadth plan and sheer plan are superimpositions of cross sections of each side on a single plane. To carry out detailed hydrodynamic evaluation such as CFD, the 2D lines plan can be used to construct the 3D model of the hull form using existing CAD tools. In addition to the hydrodynamic evaluation, these 2D offset data may be used to model the vessel in a CAD environment as part of the design and subsequent construction process. An illustration of the linkage of hull form representation is provided in Figure 3. Based on the same principle, the 2D lines plane may also be obtained through the 3D model and translated back into the offset table. The 2D hull form representation provides a versatile and useful method for geometry modification.

By working directly on offset data in the 2D domain, it eliminates a key step in existing design methods which requires 2D offset information to be re-modelled into three-dimensional (3D) surfaces manually by the designer before geometry modifications and performance evaluation can take place, thus streamlining the entire design process. This provides huge savings in manpower costs and computational resources.

<u>Two-dimensional curve morphing</u>

Curve morphing based on the 2D offset points is applied to transform the shape of hull through interpolation or extrapolation between the transverse lines of one or more existing hull forms, using the morphing equation 1 below:

$$M(t) = (1 - t) \times R_0 + t \times R_1 \qquad \text{(Equation 1)}$$

where $M(t)$ is the morphed shape, t is the morphing parameter, R_0 denotes the source shape and R_1 the target shape.

The morphing parameter is a rate of change between the source shape and the target shape. To ensure that the shape remains feasible, the morphing parameter may be restricted to between -0.1 and 1.1, inclusive of the end values. When t is between 0 and 1, the morphing is an interpolation between the source and target, while when t is less than 0 or greater than 1, the morphing is an extrapolation of the curve.

From equation 1, it may be observed when t = 0, (t) is also equal to 0 and hence the morphed shape is equivalent to source shape R_0, i.e. no change to the original shape. Likewise, when t = 1, (t) = R_1 the source will be fully transformed to the target shape. As an example, one hull line is selected from sample ship A (source) and ship B (target) at frame number 5 for both vessels. The morphing process is linear where regular and 'expected' intermediate shapes are produced. Non-linear interpolation methods such as Gaussian distribution or additional weightage, may also be applied if more random outputs (shapes) are required, and is further elaborated below. By applying equation 1 with different morphing parameters (in this case t = 0.25, 0.5 and 0.75), multiple transverse curves may be generated as illustrated in Figure 4.

By using the 2D curve abstracted from source and target vessels as provided in above example, one may observe a large number of intermediate curves may be generated by changing the morphing parameter (*t*). Other than interpolating between the source and target vessel, two 2D curve may also be extrapolated to create a new 'extended' curve. Through a 2D curve morphing method, the entire hull form or selected transverse section between the source and target vessels may be effectively transformed by just changing the morphing parameter (*t*) along the transverse frames. As compared to existing geometry modification approaches, one key advantage of this curve morphing approach is its ability to capture and modify complex shapes such as hull form using minimal design variables. To improve the versatility and flexibility of curve morphing to modify the geometry of the hull, three variations of 2D morphing are described and applied in hull form design and optimisation (HFDO), namely constant-morph, cross-morph and boundary-morph.

<u>Correspondence</u>

Prior to any morphing process, the hull coordinates for all the source and target vessels are required to be modified so as to ensure the hull form corresponds to each other. Typically no two offset tables are identical in terms of number of coordinate points or where the coordinate points are located (section and waterline levels). Therefore, the vessels may need to be regularised so that the corresponding points between source and target vessels are mapped to one another. As an example, cubic spline interpolation was used to create the same number of points across all section curves of the vessels. Cubic spline interpolation is a piecewise continuous curve which passes through each of the values in a table of points, and is represented by the following equation:

$S_i(x) = a_i(x - x_i)^3 + b_i(x - x_i)^2 + c_i(x - x_i) + d_i : for\ x \in [x_i, x_{i+1}]$ (Equation 2)

where $S(x)$denotes the spline and $[x_i,y_i]$ represents a table of points for i = 0,1,…,n for function y=$f(x)$.

As an illustration, from the initial 19 coordinate points, 11 equidistant (based on waterline or Z-axis values) coordinate points were created using cubic spline interpolation for ship A. The process was repeated for ship B to reduce the number of coordinate points from 14 to 11. In this manner, both ship A and B have the same number of coordinate points, making them correspond to each other to enable the application of 2D curve morphing, as illustrated in Figure 5.

The 2D-based cubic spline interpolation was selected for its simplicity and fast discretisation, but may result in lost accuracy and misrepresentation of the hull shape when transformed into three dimensions. Other non-linear curve fitting techniques such as B-spline surface fairing and feature-preserving smoothing may be used.

<u>Application of 2D curve morphing to hull form geometry modification</u>

To apply 2D curve morphing in hull form geometry modification, the entire 2D hull data may be simplified and mapped into a morphing scheme that represent the morphing parameter at respective frame or station number (stn). A body design, in particular ships, may be broken down into represented by a large number of frames (or cross sections), and may have hundreds of frames for each vessel. The superimposition of all the frames on the 2D lines plan may not be presented clearly. Therefore, stations are used to represent key frames (for example 20 key frames) for ease of illustration in the body / lines plan. The spacing between frames generally varies at different parts of the body design, in particular ships where it is smaller at the forward and aft of the ship. The spacing between frames may also be made equal if desired. The number of frames between each station may similarly vary or be constant. As an example, in Figure 6 the hull form may be divided into 200 frames with equal spacing to represent the entire vessel along the x-direction. The frames are further divided into 21 stations. In each station the morphing parameter (*t*) is a real-number which determines the extent to which the 2D hull lines within the frame are morphed. Figure 6 provides an illustration of the correspondence between a ship, its station number and morphing parameters. As illustrated in Figure 6, the shape of sample vessel A and B are broken up equally according to station (frame) number and assigned with a morphing parameter – *t* = 0 for vessel A (source) and *t* = 1 for vessel B (target). Using this morphing scheme, the geometry of the respective transverse frame can now be easily modified by simply changing the morphing parameters.

Constant-morph

Constant-morph is used to transform the entire hull form using the same morphing parameter (t_{CST}). By applying a constant morphing parameter (t_{CST}) across the entire length of the vessel, large number of intermittent designs may be generated through interpolating or extrapolating the offset points from 2D curve between source and target hull forms. The mathematical formula for full-morph is presented in Equation 3.

Using modified morphing expression:

$$Y(t_{CST})_{C_{x,z}} = (1 - t_{cst}) \times Y_{S_{x,z}} + t_{cst} \times Y_{T_{x,z}} \qquad \text{(Equation 3)}$$

where,

t_{cst}= morphing parameter, $-0.1 \leq t \leq 1.1$

$Y(t_{cst})_{C_{x,z}}$ = New *Y* value of the child ship at corresponding *x* and *z* coordinates

$Y_{S_{x,z}}$ = *Y* value of the source ship at corresponding *x* and *z* coordinates

$Y_{T_{x,z}}$ = *Y* value of the target ship at corresponding *x* and *z* coordinates

x = Distance from the aft perpendicular (AP) section in *X* - directions

z = Distance from baseline in *Z* - directions

The new Y values are obtained through interpolation between $Y_{S_{x,z}}$ and $Y_{T_{x,z}}$ when 0 ≤ t_{CST} ≤1. On the other hand, extrapolation between $Y_{S_{x,z}}$ and $Y_{T_{x,z}}$ are done when 0 > t_{CST} t > 1 (i.e. less than 0 or greater than 1). To ensure feasibility of the extrapolation, a constraint may be introduced here in which −0.1 ≤ t_{CST} ≤ 1.1. In some instances, some 'odd' or anomalous lines will appear during the 2D morphing process resulting in 'double hull' issue where the two different lines are duplicated on the same frame. This issue occurs mainly at the extreme bow and stern area where there is a large geometric disparity between the parent hull forms. To avoid this issue in MEC, the extreme bow and stern may preferably not be subjected to morphing procedure during the constant morph process. The boundary frame lines may each independently be a non-terminal frame line, or there is at least one or more intermediate frame lines between the terminal frame line and the boundary frame line. The terminal frame lines are the two extreme most frame lines of the body design. This allows the morphing process to avoid the extreme bow and stern to ensure the designs remain feasible.

To demonstrate the application of constant-morph, Equation 3 is applied to generate a series of 'new' hull form designs by morphing in between two existing hull forms – t_{CST} = 0 for source vessel and t_{CST} = 1 for target vessel, as illustrated in Figure 7.

Figure 7 demonstrates that the entire hull form may be modified by changing the morphing parameter (t_{CST}) uniformly across the entire length of vessel. In addition to interpolating the offset points between source and target vessels, one can also extrapolate beyond the existing vessels using constant-morph to create more 'new' designs. The morphing is done directly by interpolating or extrapolating the 2D curve at every transverse frame instead of a 3D surface or mesh. This method provides the technical advantages of the simplicity and lower computational requirement as compared to interpolating all the boundary points contained within 3D surfaces or meshes.

<u>Cross-morph</u>

To create more variations of hull form designs so as to increase the solution search space, another 2D curve morphing method involves splitting the hull forms from two different vessels at any given transverse section and combining them using a cross-morph method. This may be achieved by setting varying morphing parameter (t_{CM}) at different transverse curves along the stations or frame lines (x-planes) along the 'split' or interface sections and is shown in Figure 9. The mathematical formula for cross-morph is obtained by extending the modified morphing equation, as presented in Equations 4 to 6.

For the aft body section (from source vessel) between Aft Perpendicular (AP) and Aft Transition (AT) frame:

$$Y(t_{CM} = 0)_{x,z} = Y_{S_{x,z}} \quad , x_{AP} \leq x \leq x_{AT} \qquad \text{(Equation 4)}$$

For forward body section (from target vessel) after Forward Transition (FT) frame and Forward Perpendicular (FP):

$$Y(t_{CM} = 1)_{x,z} = Y_{T_{x,z}} \quad , x_{FT} \leq x \leq x_{FP} \qquad \text{(Equation 5)}$$

For mid-body section between Aft Transition (AT) and Forward Transition (FT) frames:

$$Y(t = x_{TS} \times W)_{TS_{x,z}} = (1 - t) \times Y_{S_{x,z_{AT}}} + t \times Y_{T_{x,z_{FT}}}$$

$$\text{for } x_{AT} \leq x_{TS} \leq x_{FT} \text{ , } W = 0.1 \times (x - x_{AT}) \qquad \text{(Equation 6)}$$

where,

t_{CM} = morphing parameter, $0 \leq t_{CM} \leq 1$

$Y_{S_{x,z}}$ = *Y* value of the source ship at corresponding *x* and *z* coordinates

$Y_{T_{x,z}}$ = *Y* value of the target ship at corresponding *x* and *z* coordinates

$Y(t = x_{TS} \times W)_{TS_{x,z}}$ = New *Y* value of the transition section at corresponding *x* and *z* coordinates

x = Distance from AP section in *X* - directions

z = Distance from baseline in *Z* – directions

x_{AT} = x frame at the aft transition section

x_{FT} = x frame at the forward transition section

x_{TS} = x frame between x_{AT} and x_{FT}

x_{AP} = x frame at the aft perpendicular (AP) section

x_{FP} = x frame at the forward perpendicular (FP) section

W = weightage

Using sample vessel A and B as example, the body of both vessels are 'cut' at mid-ship (middle body) and combined as illustrated in Figure 8. From Figure 8, it may be observed that it may not be a feasible model solely by joining two unrelated hull forms together as there is a sudden change in the mid body which results in an unsymmetrical forward and aft body. However, by applying a gradually changing (for example linear) morphing parameter (t_{CM}) on multiple curves along different stations (X-axis) (the transition section), a smooth transition may be created effectively from the aft section of ship A to the forward (fwd) section of ship B. Figure 9 and 10 show how the cross morph is applied to the mid body of the vessel by changing the morphing parameters (t_{CM}) linearly. In Figure 9 the morphing parameter changes from 0.25 to 0.75 at station 4.5 to 5.5. In Figure 10 the morphing parameter changes from 0.1 to 0.9 at station 3 to 7 (highlighted) of the vessel. Note there are no changes to the lines of ship A (source) when t_{CM} = 0 and vice versa for ship B (target) when t_{CM} = 1. Thus, it may be seen that the cross-morph may be applied with different variation of the morphing parameter and with different length of the transition section.

The hull shape may be changed effectively towards more of vessel A or vessel B by varying the morphing parameters (t_{CM}) at different parts of the vessel, as illustrated in Figure 11. There are no changes to the lines (or shape) of aft body of vessel A when morphing is applied to the forward body of vessel B (Figure 11(a)) and likewise no changes to forward body of vessel B when morphing is applied to the aft body of vessel A (Figure 11(b)).

The cross-morph method allows two different hull bodies to be “joined” together smoothly. By varying the morphing parameter (t_{CM}) at different transverse frames, one can choose which attributes the curve should be transformed, whether it should be more of vessel A (toward t_{CM} = 0) or vessel B (towards t_{CM} = 1). This provides great flexibility to change the hull shape effectively at any location of the ship and yet maintain a smooth transition. The number of transition frames depends on the shape difference between the joining sections. For example, the greater the difference in shape and/or size between the existing parents, the larger the number of required transition frames. In the example below, two very different vessels are combined and the transition frames extend from the forward to aft section of the vessel, leaving very little of the parent ships A and B untouched.

Using the same principle, one may also ‘cut’ and join two or more vessels at different sections such as vessel A aft body to vessel B mid body to vessel C forward body. By changing the source and target model, the vessel can be effectively morphed into a combination of more than two vessels – as illustrated in Figure 12 and Figure 13. Figure 13(a) shows a sample vessel C body plan while Figure 13(b) shows a combination of vessel A aft body, vessel B mid body (from Figure 11) and vessel C forward body. On top of morphing two or more hull forms together into one hull concept, cross-morph can also be applied by mixing different combinations. For example, instead of joining vessel A-B and B-C, one can also join up vessel A-C and C-B, etc. While cross-morph may be simple to apply directly for geometrically similar ships, it may also be applied to ships sizes that are vastly different. In some instances, some ‘odd’ or anomalous lines may appear during the 2D morphing process resulting in a ‘double hull’ issue where the two different lines are duplicated on the same frame. This issue occurs mainly at the extreme bow and stern area where there is a large geometric disparity between the parent hull forms. To avoid this issue, the extreme bow and stern may preferably not be subjected to morphing procedure during the cross-morph process. The boundary frame lines are each independently a non-terminal frame line, or there is at least one or more intermediate frame lines between the terminal frame line and the boundary frame line. This allows the morphing process to avoid the extreme bow and stern to ensure the designs remain feasible.

Cross-morph provides a method of obtaining a new body design, in particular a hull design. The method comprises performing a crossover combination of two or more body designs to provide the new body design. The method may further comprise rescaling at least one of the two body designs to fit the other body design. As an example, the cross morph may utilise Equations 4 to 6 as shown above.

Single point cross morph application example

Two existing vessels with vastly different dimension or hull forms may also be combined by cross morph. In this example, a volume carrier (Very Large Crude Carrier – VLCC) and an offshore vessel (pipe-laying) are combined using the cross-morph approach. The principle dimensions for both vessels are provided in Table 1 and the isometric views of both hulls are illustrated in Figure 14. Figure 14(a) and 14(b) show the pipe-laying vessel and VLCC respectively.

Table 1: Principle dimensions of two existing vessels

	VLCC / m	Pipe-laying / m
Length overall (Loa)	327	182
Length between perpendiculars (Lpp)	314	168
Breadth (B)	58	46
Height (H)	31	23
Design draft (T)	20	11

A possible way to generate new hull combinations or variations is by “splitting” both vessels in the mid-ship section and combining them as illustrated in Figure 15, with the shaded plane being the intersection point (plane) between both vessels. It may be observed that this may not be a feasible model as there is a sudden change in the mid body which results in an unsymmetrical forward and aft body. However, by applying a gradual morphing parameter (t_{CM}) on multiple curves along different stations (X-axis) using the cross-morph method, a smooth transition may be created from aft section of ship A to forward section of ship B. The resultant design is shown in Figure 16. Figure 16(a) shows the wire mesh diagram of the vessel in three sections – the forward section of the pipe-laying vessel (vessel A), the transition section (or mid body) and the aft section of the VLCC (vessel B). The cross-morph is applied to mid body of the vessel by setting gradual changing morphing parameters (t_{CM}) of 0.1 to 0.9 at station 1 to 9 of the vessel. There are no changes to the lines of ship A (source) when t_{CM} = 0 and for ship B (target) when t_{CM} = 1. Figure 16(b) shows the 3D surface diagram of the combined vessel body design. Due to the large difference in dimensions of both parent ships, the transition section may be a significant portion of the combined design, with a small original section of each parent. In this example, no scaling of one vessel to fit the other vessel is done, however, when multiple iterations of the cross-morph with parent hull forms whose principle dimensions differ greatly, the possibility of infeasible designs may increase.

This example demonstrates how two different hull bodies can by 'joined' smoothly together using cross-morph technique. By varying the morphing parameter (t) at different transverse frame, one can choose which attributes the curve should be transformed, whether it should be more of ship A (toward $t_{CM} = 0$) or ship B (towards $t_{CM} = 1$). This provide great flexibility to change the hull shape effectively at any location of the ship and yet maintain a smooth transition for feasible hull design. To improve the shape changes in the transition area of both vessels, an additional smoothing function may be incorporated and is elaborated below.

Two-point cross-morph application example

Three different vessel types may be combined into one hull form through two-point cross-morph. This function allows the segregation of hull form into three main sections – stern (aft) section, mid-section and bow (forward) section, and enable the creation of more hull form designs through a mix-and-match process. This may be achieved by rescaling using a linear proportional approach to resize the vessels to similar or same principle dimension, following which, the three vessels are 'split' into three separate sections and 'join' together using cross-morph and is shown in Figure 17. Similar to single point cross-morph example above, the rescaling is optional but may minimise infeasible designs by avoiding drastic changes in the transition frame. Here the morphing parameter (t_{CM}) for ships A, B, and C are set to 0, 1 and 2 respectively. The morphing parameters in the transition sections between each ship may be set to be linear incremental values to gradually morph from one ship section to the next ship section.

In this example, the three ships are a container ship, a bulk carrier and an oil tanker. The rescaling is done to the dimensions of the oil tanker, and the aft body of the container, mid body of the bulk carrier and the forward body of the oil tanker are joined together as showing in Figure 18. Cross morphing is performed to join the aft body of the container and the mid body of the bulk carrier and the mid body of the bulk carrier and the forward body of the oil tanker. It will be appreciated that the existing vessel may be "split" and "join" as desired or required, and is not limited to the specific examples.

The cross-morph method is versatile and allows the crossover combination of two or more existing body designs with different functions and sizes. This is very useful when applied into geometry modification for HFDO which may create more different types of hull form combinations and unique designs. A limitation of using this geometry modification approach

is the new designs are closely linked to the parent design. To overcome this limitation, more existing vessel designs may be used, or created from scratch to morph and generate new designs. For example, different design types of hull form in the way of three main sections of the vessel - stern, mid and bow section are illustrated in Figure 19. The cross-morph approach increases the solution space and provides another function within HFDO to create more innovative hull form.

Boundary-morph

An overview of the boundary morph method 100 is shown in Figure 1. The computer implemented method 100 may be used to generate a new body design for a new vehicle. The method 100 may be performed by a processor within a computing system. The method 100 includes providing an initial body design of a vehicle, in particular a hull design, in a two-dimensional space with a plurality of frame lines in block 105; selecting two boundary (a first and a second) frame lines in the initial body design in step 110; selecting a reference frame line between the two boundary frame lines in block 115; selecting a morphing parameter, the morphing parameter is a rate of change between the boundary frame line/s and the reference frame line in block 120; based on the morphing parameter, modifying the initial body design from the reference frame line towards either or both of the boundary frame lines in block 125; and generating the new body design based on the morphing parameter in block 130. The initial body design may be converted into the two-dimensional space and multiple frame lines using the offset table as explained. The frame line may also be called a curve in the two dimensional space. The boundary frame line may be preferably selected by the user or randomly selected by a processor. The boundary frame lines may be adjacent to each other such that one is the boundary (target) curve and the other is the reference (source) curve. The boundary frame line may be the terminal frame line. The terminal frame line refers to either of the 2 extreme frame lines of the body design (one each from the forward and aft sections). In some instances, some ‘odd’ or anomalous lines will appear during the 2D morphing process resulting in ‘double hull’ issue where the two different lines are duplicated on the same frame. This issue occurs mainly at the extreme bow and stern area where there is large geometric disparity between the parent hull forms. To avoid this, the extreme bow and stern may preferably not be subjected to morphing procedure during the boundary-morph process. The boundary frame lines may be a non-terminal frame line, or there is at least one or more intermediate frame lines between the terminal frame line and the boundary frame line. This allows the morphing process to avoid the extreme bow and stern to ensure the designs remain feasible. In an example, the boundary frame line/s is proximal to the terminal frame line. Thus, the first boundary frame

line may be a frame line near the terminal frame line in the forward section of the body design, and the second boundary frame line may be a frame line near the terminal frame line the aft section of the body design. This allows the two boundary frame lines to bound a region which is a substantial portion of the whole body design, and may be at least 50%, at least 60%, at least 70%, at least 80%, or at least 90% of the entire body design. The region bounded by the two boundary frame lines may preferably be at most 95% of the entire body design or 90% of the entire body design. In an example, the two boundary frame lines may bound 50% to 95% of the entire body design, or bound 60% to 95% of the entire body design, or 70% to 95% of the entire body design, or 80% to 95% of the entire body design, or 90% to 95% of the entire body design. In another example, the two boundary frame lines may bound 50% to 90% of the entire body design, or bound 60% to 90% of the entire body design, or 70% to 90% of the entire body design, or 80% to 90% of the entire body design. This allows for extensive modification of the body design but in a simple and efficient manner. Further, by avoiding the extreme ends of the body design, unfeasible designs are minimised or eliminated.

The reference frame line may be selected by the user or preferably selected randomly by a processor which provides an advantage of generating designs without an inherent bias users may possess and inadvertently imbue into the design. Similarly, the morphing parameter may be user defined or randomly selected by the processor, and preferably within a range to avoid unfeasible designs. The processor subsequently applies the morphing parameter to modify the selected reference frame line towards at least one of the boundary frame lines, concurrently or independently. In most situations, there will be at least one intermediate frame line between the reference frame line and the boundary frame line. To ensure that the design remains smooth and feasible, the at least intermediate frame line/s may be adjusted based on a modified morphing parameter. For example, the morphing parameter of the intermediate (or adjacent) frame line/s increases or decreases gradually from the reference frame towards the boundary frame line, depending on whether an inward shift or an outward shift is required. The modified morphing parameter is thus dependent on the (value of the) morphing parameter at the reference frame line. In an example, the morphing parameter linearly increases or linearly decreases. The modified morphing parameter may be obtained from the morphing parameter by a weightage which is dependent on the location of the intermediate frame line in question with respect to the total number of frame lines between the reference frame line and the boundary frame line. A smoothing factor may be used to ensure the frame line/s adjacent to the selected reference frame line may be adjusted together with the reference frame line to ensure a

smooth curvature in the new body design to ensure that the new body design is feasible. Three or more boundary frame lines may be defined to break the body design into smaller sections for the modification, i.e. each section is between two boundary frame lines.

In another example, a non-linear weightage may be used and may be applied to remove need for smoothing factor. For example, the linear function may be broken into 3 sections – a first section near the near boundary frame (small difference, low weightage), a second mid-section (large difference, mid weightage), a third section near the reference frame (small difference, high weightage). Advantageously, this reduces the curvature / shape difference near the boundary and reference curves to improve the feasibility and smoothness for better hydrodynamic performance.

The constant-morph and cross-morph each requires two or more existing body designs or parent vessels in order to interpolate or extrapolate to produce new designs. In contrast, the boundary-morph method utilises only a single existing body design to provide a new body design, by interpolating between the transverse section and the extreme boundary of forward, mid and stern section of the original or principle vessel.

An example of the extended morphing equation that may be used for boundary-morph is as follows:

For morphing the reference frame between the Mid-Boundary (MB) curve (source) to the Forward or Aft Boundary (F/AB) curve (target):

$Y(t = x_R \times W)_{R_{x,z}} = (1 - (t \times S_{TS})) \times Y_{S_{x,z}} + (t \times S_{TS}) \times Y_{T_{x,z}}$

where $W = 0.02 \times (x - x_{AB})$ when $x_{AB} \leq x \leq x_{MB}$ and $W = 0.02 \times (x - x_{MB})$ when $x_{MB} \leq x \leq x_{FB}$ (Equation 7)

For morphing adjacent frames between the Reference (R) curve (source) to the Mid-boundary (MB) or the forward and aft boundary (F/AB) curve (target):

$Y(t = x_A \times W)_{A_{x,z}} = (1 - (t \times S_{TS})) \times Y_{S_{x,z}} + (t \times S_{TS}) \times Y_{T_{x,z}}$

Where $W = 0.04 \times (x - x_R)$ when $x_R \leq x \leq x_{MB}$ and $x_R \leq x \leq x_{FB}$,

$W = 0.04 \times (x_R - x)$ when $x_{AB} \leq x \leq x_R$, and

$W = 0.04 \times (x - x_{MB})$ when $x_{MB} \leq x \leq x_R$ (Equation 8)

subject to $0.2 \leq t \leq 0.8$ and smoothing factor, $S_{TS} = 1 - \frac{Y_{TS}}{B_{max}}$ (Equation 9)

where $Y(t)_{R_{x,z}}$ is the new *Y* value for the reference curve at corresponding *x* and *z* coordinates, $Y(t)_{A_{x,z}}$ is the new *Y* value for adjacent curves at corresponding *x* and *z*

coordinates, $Y_{S_{x,z}}$ is the *Y* value for the reference (source) curve at corresponding *x* and *z* coordinates and $Y_{T_{x,z}}$ is the *Y* value for the boundary (target) curve at corresponding *x* and *z* coordinates. x_A is the x coordinate of the adjacent frame between the reference frame and boundary frames, $x_{F/AB}$ is x frame at the forward or aft boundary section, x_R is x frame at the reference frame section and x_{MB} is x frame at the mid boundary section. W is the weightage, Y_{TS} is the Y value of the transition section between the two boundaries and B_{max} is the maximum ½ breadth.

From Equations 7 and 8, the weightage factor allows a gradual increase of morphing parameter t until it reaches the target curve. In the case of the smoothing factor, shown in Equation 9, it is applied to inject the non-linearity function into the morphing function so as to ensure smooth transitioning between the X-directions. This is achieved by benchmarking the Y-value of the selected frame with respect to the largest Y-value of the vessel (maximum half-breath) at any given X-location.

The weightage (W) applied to vary the morphing parameter depends on the position of the curve. For example, full weightage may be applied to only the reference curve and reduces for the neighbouring curves all the way until the boundary curve has zero weightage and is not modified. The boundary-morph method allows the entire hull form to be modified by morphing the reference frame line (curve) from the reference frame line to the boundary frame line with the intermediate frame lines modified using varying weightage and smoothing factor as shown.

Figure 20 shows an example of the boundary-morph method. Firstly, three boundary curves are selected, one forward boundary curve (station 10), one aft boundary curve (station 0) and one mid boundary curve (station 5). This splits the hull into two sections - forward and aft as shown in Figure 20. In the next step, depending whether it is inward or outward shifting, the morphing parameter *t* for respective boundary curves is changed accordingly. As an example, for modifying the aft section, outward shifting may be performed by setting the aft reference curve as *t* = 0 and the mid boundary curve as *t* = 1. On the other hand, inward shifting may be performed by setting aft reference curve as (*t* = 0) and aft boundary curve as (*t* = 1). After which, this selected reference curve is morphed towards either of the boundary curve (aft or mid) by changing the morphing parameter *t* accordingly.

The same principle applies to modifying the forward section where outward shifting is performed by setting forward reference curve as t = 0 and mid boundary curve as t = 1. Similarly, inward shifting is carried out by setting forward reference curve as t = 0 and forward boundary curve as t = 1. By assigning different weightages on the morphing parameter t of adjacent curves, the entire forward or aft section of the hull can be modified into a more slender or fuller shape by changing the morphing parameter t. This example uses three boundary frames (curves or frame lines), it is also possible for the mid boundary curve to be omitted, or for either the forward or aft boundary curve to be omitted to use the boundary-morph method. For example, if the forward and aft boundary curves are selected, the reference frame line will thus be any frame line between the forward and aft boundary curves.

The reference curve and morphing parameter may each independently be set by a user or randomly set by a processor, and may be further restricted within certain limits to avoid unfeasible designs.

<u>Boundary morph application example</u>

An example of how a hull form of a container vessel may be modified using boundary-morph is shown in Figure 21. Firstly, three boundary curves are selected as forward curve (station 10), mid curve (station 5) and aft curve (station 0) as shown in Figure 21. The settings of the morphing parameter (t) for each curve at the respective stations are also provided.

For the first scenario shown in Figure 22(a), a forward reference curve is selected at station 7.5 and morphed towards forward boundary curve at station 10 by setting the morphing parameter to t = 0.5. At the same time, it may be observed that the neighbouring curves of the forward reference curve were also changed concurrently, preferably through a smoothing factor (Equation 10) that was applied to change the morphing parameter t gradually for each curve corresponding to the morphing scheme. This resulted in a more slender hull form at the forward section of the vessel.

Using the same concept, the aft section was modified by selecting the aft reference curve (station 2.5) and morphed towards the aft boundary curve (station 0) with the morphing parameter set to t = 0.5, in the second scenario shown in Figure 22(b). The first two scenarios here are an example of the inward shifting.

This resulted in a more slender hull form at the aft section. In third scenario shown in Figure 22(c), the same forward reference curve (station 7.5) is morphed towards the mid boundary curve (station 5) with the morphing parameter set to t = 0.5, resulting in a much fuller hull form at forward section. Likewise in the fourth scenario shown in Figure 22(d), the aft section (station 2.5) was morphed towards the mid boundary curve (station 5) using a morphing parameter of t = 0.5. This resulted in a fuller hull form in the aft section. The latter two scenarios are an example of the outward shifting.

The four scenarios demonstrated that boundary-morph may be applied effectively to modify the shape of the hull using only one principal vessel. This is achieved by introducing different weightages to neighbouring curves of the reference curve and morphing them towards the boundary curve.

When applied to HFDO, geometry modification using 2D curve morphing may help to reduce the computation time significantly as compared to 3D surface modification. The three 2D curve morphing methods described allows modification of the shape of hull in a more automated yet wide-ranging manner. Constant-morph enable the entire hull form to be modified using only one design variable - morphing parameter (t_{CST}). Cross-morph enables the joining of two or more hull forms in a seamless manner. Boundary-morph allow geometry modification of hull form using only one reference vessel. These geometry modification methods are very useful when applied, alone or in various combinations, to an optimisation process such as HFDO as it enables a fully automated geometry modification process.

The morphing parameters for each of the method described may be generated randomly within the constraint set for feasibility reason. An advantage with having random selection is to increase the design diversity and search space for the method to explore and thereby increasing the probability to find more optimal designs. The functionality of the morphing parameter (t) is the same for the three morphing methods but the value varies based on the 3 different equations.

The boundary-morph method advantageously only requires one design variable (morphing parameter) and one body design. By varying the morphing parameter, the curve may be modified concurrently in two dimensions or coordinates. The curve may also be modified in the remaining dimension depending on the transition section affected. The boundary-morph method may allow for large shape transformation and variations and may be applied with

minimal to negligible user input. With modifying a substantial part of the hull design, the use of three boundary curves (forward, mid and aft) may be preferable since the forward and aft sections of the hull designs often have different hydrodynamic and/or aerodynamic requirements depending on the particular vehicle body design, and may provide more feasible designs.

Genetic algorithms and Non-sorting genetic algorithm (NSGA-II)

Genetic Algorithms (GA) is a heuristic search method based on the Darwinian theory of natural selection and the "survival-of-the-fittest" principle. GA is a subset of Evolutionary Computation (EC), a family of nature-inspired algorithms for global optimisation. GA works based on the principle of genes and chromosomes. Using genetic operators such as selection, crossover and mutation, information represented by genes are exchanged between chromosomes over several iterations, typically with fitter solutions replacing weaker ones. This will eventually lead to a set of optimal solutions, which are represented in the form of a Pareto frontier. A Pareto frontier is a set of solutions where no solution is better off (or more superior) than the others at any given point within the solution space. Compared to other EC approaches such as Evolutionary Programming (EP) and Particle Swarm Optimisation (PSO), GA can search within a large solution space within a relatively short time.

To fully appreciate the working principles of GA, it is important to first understand how it represents (maps) an optimisation problem. A solution in the actual problem space is termed a phenotype and its corresponding representation in the GA space is termed a genotype. For example in design optimisation, a phenotype may be a possible solution to the problem such as an object which may be represented in the form of either integer or float or bit string in the GA or genotype space. In GA, this representation is termed a chromosome and is made up of building blocks known as genes. Figure 23 provides an illustration of this concept and the encoding and decoding of a solution.

Once the phenotype – genotype mapping is established, information exchange takes place between chromosomes through genetic operators, namely, selection and replacement, crossover and mutation. This takes place over several iterations, typically with better solutions replacing weaker ones, eventually leading to a set of optimal solutions at the end of the optimisation process. The phenotype-genotype mapping of a problem is thus a crucial step in GA as an incorrect or inappropriate representation of the problem will result in failure of the optimisation. A GA typically has six key steps, as shown in Figure 24.

Step 1 – Initial population: The first step of the GA is to initialise a group of population as the initial parents. Similar to biological system, each parent is made up of many different genes that forms into a chromosome. The genes may be represented in either binary or numerical forms.

Step 2 – Fitness evaluation: The initial population goes through an evaluation process to determine the fitness value for each individual. The evaluation method will be based on the objective function defined in the optimisation problem.

Step 3 – Selection: Selection process take place to pair individuals together based on their fitness value to produce the next generation or child (solutions). In GA, there are several types of selection process which includes roulette wheel, tournament selection and linear ranking.

Step 4 – Cross-over: The regeneration process will take place in a cross-over process where part of each parent genes will be passed onto the new child (solution). This cross-over process can be either single or multiple point cross-over and adjusted by different ratings which will affect the diversity of new solution generated.

Step 5 – Mutation: Mutation process take place to infuse a unique trait into the child through minor modification of the gene that are apart from the parents' gene. This process helps to introduce new elements into the child (solution) and yet enables the retention of the good genes created from the cross-over process.

Step 6 – Repeat process: In the next generation, these newly formed child (solutions) will grow to become adults and forms a new population as parents. The whole process will be repeated, creating generation after generation of child (solutions) which will become stronger as part of the evolutionary process.

NSGA-II is based largely on the working principles of the original GA but possesses additional features, namely, non-dominated sorting and a crowding distance measure to enhance the search process. When compared to standard GA, Niched-Pareto Genetic algorithm (NPGA) or NSGA-I [182], NSGA-II is particularly useful for multi-objective problems as it helps the population reach the true pareto-optimal front and sustains the spread of solutions even with large numbers of generations. It searches a design space more effectively, leading to more diverse and creative solutions.

A basic illustration of non-dominated selection and crowding distance within NSGA-II is provided in Figure 25. The key steps in NSGA-II are:

Step 1 - Gather the same number of parent population (from previous generation) and the new offspring population to form the initial population.

Step 2 - Sort the population into different Pareto fronts according to non-domination level (for example, F1 is the best level followed by F2 and so on). Apply binary tournament selection to randomly select two solutions from the current population and select the better solution with respect to non-domination ranking.

Step 3 – Compare the solution within the same non-domination front using crowding distance to measure the density of neighbouring solutions.

Step 4 - Create the next generation by copying the best solutions (elitism) from the mixed population of parents and off-springs. Solutions that are not copied to are rejected.

By incorporating elements of the morphing methods described above with the GA and NSGA-II methods, a morphing evolutionary computation (MEC) method may be developed. The MEC method allows a wide range of body designs, in particular hull form designs, to be created in a short period of time with a lower computational power requirement to allow an optimal hull form to be arrived at and further manufactured. An overview of the MEC approach is shown in Figures 26, 27 and 28. In Figure 26, the design exploration starts from the problem formulation, followed by initialisation of the method using a hull form library and constant morph of existing hull designs if necessary, fitness evaluation of the hull designs in the library, selection of random pairs from the library, cross-over combination of the selected pair of designs, mutation of the combined design, replacement and determination if the termination objectives are reached or the process repeats. A difference between the MEC methods described herein and existing NSGA-II methods is in the crossover and mutation operator, where real-value chromosomes (morphing parameters) are used to change the geometry of the vessel and create new solutions.

MEC is developed to optimise the shape of the hull, and other vehicle bodies, based on the transverse hull lines of proven hull designs automatically. Unlike conventional geometry modification and optimisation approaches which require the designer to input the shape variation directions and degree of changes for the optimiser to explore, MEC allows automatic geometry variations based on proven designs which enables the generation of feasible designs with minimum to negligible human intervention.

<u>Problem formulation and initialisation</u>

In most optimisation problems, formulating the right objectives and constraints are paramount to the success of the optimisation. This is particularly true for complex problems

such as hull form optimisation. Therefore, it is important to identify input design specifications as well as objective functions before the optimisation commences. These include the ship type, principal dimensions such as Length between Perpendiculars (LPP), beam (B) and draft (T). Depending on the design specifications, objective functions may include minimising resistance and/or seakeeping. In addition, proven designs stored in the hull form library that are used as starting points for the optimisation are prepared during initialisation.

Objective Function

In real world applications, there are two main types of optimisation problems - single and multi-objective. The main goal of single objective problems is to find the 'best' solution to a design criterion. This could correspond to the minimum or maximum value of the objective function and may be formulated as shown in Equation 10.

Minimise or maximise f(x),

subject to

$$h_k(x) = 0, \qquad k = 1, \dots, K$$
$$g_j(x) = 0, \qquad j = 1, \dots, J$$
$$x_{nl} \leq x_n \leq x_{nu}, \qquad n = 1, \dots, N \qquad \text{(Equation 10)}$$

where f is the objective function, K is the equality constraint, J is the inequality constraint, x represents the vector of design variables and x_{nl} and x_{nu} are the lower and upper bounds of the xth design variable, x_n, respectively.

Conversely, multi-objective optimisation problems usually deal with conflicting objectives where there is no unique global solution but a set of solutions. In general, a mathematical problem to multi-objective optimisation can be represented as shown in Equation 11:

Minimise or maximise $f_i(x), \qquad i = 1, \dots, I$

subject to

$$h_k(x) = 0, \qquad k = 1, \dots, K$$
$$g_j(x) = 0, \qquad j = 1, \dots, J$$
$$x_{nl} \leq x_n \leq x_{nu}, \qquad n = 1, \dots, N \qquad \text{(Equation 11)}$$

where f_i represents the objective functions, K is the equality constraint, J is the inequality constraint, x represents the vector of design variables and x_{nl} and x_{nu} are the lower and upper bounds of the xth design variable, x_n, respectively.

Constraints

Design constraints determine the minimum and maximum allowable limits and thus have a huge influence on the design solution space. Any design that does not meet the constraints

will be deemed infeasible, as illustrated in Figure 29. Some examples of design constraints in hull form design optimisation include principal dimensions such as length, breath and draft, displacement, deadweight, speed and cargo capacity. Principal dimensions and displacements are preferably considered in MEC. In MEC, only feasible solutions are carried over to the next generation while infeasible solutions are discarded.

An initial population (or set) of body designs (hull form in case of ship) are required (i.e. at least two body designs are required). This may be obtained from existing body designs, for example stored as a library in a database 205 as in Figure 27, or created from scratch. If the database 205 does not contain sufficient existing designs, a constant-morph process may be performed on at least two of the existing designs to generate a new hull design. The constant-morph approach expands the population through interpolating or extrapolating the hull form of existing designs. The designs (from the library and/or from the constant morph modification) form an initial population 215. As an example, the library in Figure 27 contains 10 hull designs, and 2 hull designs are obtained by the constant-morph modification method to form an initial population (or set of initial solutions) with 12 hull designs. The advantage of using existing designs is the assurance of their performance which are validated to meet design objective and helps to shorten the design cycle. On the other hand, it is recognised that the improvements are often incremental. Another alternative is to model a new hull form from scratch which will allow more freedom of design thereby allowing the creation of more innovative hull forms. Each individual hull design in the initial population may be mapped with the phenotype-genotype mapping.

<u>Linear proportion approach</u>

Based on the design requirement set during problem definition, the existing vessels may be scaled up or down by applying linear proportion approach to modify the hull form according to desired length, beam and draft. Linear proportion is one of the simplest methods of hull shape transformation where the breadth and draught are changed proportionally to keep the form similar to basic form. The linear proportion method is illustrated in Figure 30.

The general formula for the linear proportion method is provided below:

$h_1 = \frac{h \times H_1}{H}$; $b_1 = \frac{b \times B_1}{B}$ (Equation 12)

Where H and B is the overall height and half-breath and h and b is the sectional height and half-breath of the scaled-down vessel and $H1$ and $B1$ is the overall height and half-breath of the vessel and h_1 and b_1 is the sectional height and half-breath of the scaled-up vessel.

Phenotype to Genotype mapping

Candidate solutions (hull forms) may be represented in the genotype space as real-valued chromosomes. As described above, the hull of the vessel is divided into x frames, each corresponding to a gene in the chromosome. For example, in Figure 31 each gene contains two variables, namely, the station number and a morphing parameter (*t)*. The station number represents the transverse frame in the X-plane and corresponding *t* value, which changes the hull geometries according to the 2D curve morphing methods described.

Incorporating the morphing scheme into the phenotype-genotype mapping for MEC enables the hull shape to be transformed globally by simply changing the morphing parameter *t* at various stations along the entire vessel when coupled with a GA. This unique mapping process helps to map the entire 2D offset table of the hull into a simple representation using the morphing parameter *t* for each station and provides a simple yet direct representation of the ship geometry.

In other applications of GA in hull form optimisation, the mapping is typically represented by the design variables in the form of real or binary strings used to modify the hull geometry as defined by the designer. For example, some methods use an indirect mapping method which employs multiple parameters such as length, breath, height (or x,y,z coordinates) to represent and modify the hull geometry, where the modifications are very restricted or limited. Some other methods use binary codes (00100111) to represent different geometry features. The challenge arises as the shape variation increases, a greater number of geometry parameters needs to be considered and thereby increases the overall computation time when coupled with the optimisation and evaluation process. The phenotype-genotype mapping method allows large shape variation by changing only one design parameter (*t)* and hence is very flexible and efficient when used in HFDO.

GA parameters

During initialisation, several GA parameters are specified. These parameters include the crossover and mutation rates, elitist size, population size and number of generations. Crossover and mutation rates determine the probability of information exchange between the selected chromosomes. The population size is the number of chromosomes generated

in every generation. The number of generations determines how many times the process repeats before terminating. Elitist size determines the number of child solutions (as a factor of population size) to be carried over to the next generation. These settings have a strong impact on the outcome of the entire optimisation process and need to be adjusted accordingly to the optimisation problem. An example of GA settings is provided here.

No. of generations: 100
Population size: 10
Crossover rate: 0.9
Mutation rate: 0.9
Elitist size: 0.1× population size

Due to the limited number of initial solutions available, the initial population size was set to 10 and 100 generations to allow sufficient time for the new solutions to grow and expand without pre-matured convergence. High crossover and mutation rates of 0.9 were set to ensure a higher chance of new solutions being generated to increase the variety of solutions. In addition, a small percentage of the best individuals in the population may be carried forward to the next generation via elitism to ensure that good individuals are preserved. However, it should be noted that crossover and mutation rates that are too high (e.g. 1.0) may be disruptive and the search may not converge.

Selection and replacement

Selection is a process of picking individuals that will be used in the reproduction process for generating new solutions. The principle is to always select good solutions to increase the chances of obtaining better individuals. Current selection methods include roulette wheel, linear ranking and tournament selection. Roulette wheel randomly selects individuals according to their fitness values. An advantage of this method is that it preserves the diversity of the population by giving every individual a chance to be selected. However, it tends to have premature convergence. In tournament selection, individuals will compete in the entire population based on their fitness values to be selected as a parent. Its simplicity and efficiency make it the most popular selection method. However, this method results in great reduction in diversity as individuals with the highest fitness values tend to be selected constantly while those with low fitness values will lose out either in the beginning or at immediate stages. Linear ranking selects parents by ranking the fitness of the individuals. This selection method addresses the issue of premature convergence but requires high computation time and hence not favourable for the complex optimisation problem. There are other selection methods that do not depend on the fitness of individuals. One such

method is the random selection method which selects a parent on a purely random basis and provides equal probability for every individual to be selected in every generation. In an example, considering that all parent or existing vessels in the hull form library are of proven designs and useful, random selection may be preferred.

Replacement methods are used to determine if the newly created solution will be used to replace some, all or none of the current solutions. There are different replacement methods that are applied to GA. These include tournament selection, deterministic crowding, first-in-first-out, conservative strategy and elitism. In an example, replacement is applied using the elitism approach. Elitism is based on the principle of the survival-of-the-fittest where best solutions in each generation are preserved and carried forward to the next generation in hope of producing better solutions. The replacement method for building the next generation of candidate solutions was compared between GA without elitism and NSGA-II with elitism. Figure 33 shows a comparison when the two methods were applied to a minimisation problem.

It may be observed from Figure 33(a) that the solutions found throughout the optimisation process were concentrated around the centre of the initial population. This means that there is little diversity and solutions found may not be better than the initial designs. When elitism was implemented, the solutions obtained as shown in Figure 33(b) converged towards the lower left corner of the solution space. It may thus be concluded that preserving the best individuals throughout the optimisation process could lead to better solutions at the end of the search.

<u>Crossover</u>

Crossover is an important operator in GA where the chromosomes of two parents are combined to form a new chromosome of the child. The principle of this operator is to create new individuals by mixing the good genes of their parents which will subsequently lead to fitter individuals. An important parameter for crossover in GA is the crossover rate. Crossover rate determines the percentage (or probability) of the solution going through crossover, with a range from 0 to 1. A crossover rate of 0 means that none of the solutions will go through crossover while 1 means all solutions will go through crossover.

In MEC, cross-morph is applied in crossover through the encoding scheme to create new (child) solutions. To demonstrate the effects of different crossover rates in MEC, a comparative study was carried out using crossover rates of 0.1 to 1.0 in incremental values

of 0.1 (405, 410, 415, 420, 425, 430, 435, 440, 445, 450 respectively) and a mutation rate of 0 to evaluate the effects of crossover only. Six initial (existing) designs were used to form the initial population. The results obtained from this study are shown in Figure 34.

Figure 34 shows that the resistance of the solutions reduced as the crossover rate increased. The results may be influenced by multiple factors - random selection of the crossover-point and random selection of the initial parents for combination, which give different results. For example, crossover rates of 0.1 to 0.3 (405, 410, 415) resulted in higher resistance values than crossover rate of 0.7 to 1 (435, 440, 445, 450). This demonstrates that the higher the crossover rate, the higher probability the solutions will go through crossover and create new solutions that perform better. Next, it may be observed that the solutions in almost all crossover settings converge before the 20th generation and the search stagnates thereafter. This demonstrates that there are limited new solutions created. This may be due to a lack of diversity in the solutions created in the crossover. This is a reasonable result considering that there are only six vessels in the initial population which limits the number of new shapes that may be created using cross-morph. Nevertheless, this example demonstrated the ability of crossover in MEC to generate new designs (solutions) with better overall performance.

<u>Mutation</u>

Mutation is the next reproduction process in the GA. Here, new genes created from crossover are randomly perturbed to produce new genetic structures. In the phenotype space, this may be seen as changes made to the object such as the hull. Similar to crossover, mutation in GA is controlled by the mutation rate and it determines the probability of the solutions going through mutation. By mutating a chromosome sparingly, new variations are introduced into existing solutions to form new ones which will still retain some traits of the solution. In MEC, the boundary-morph method may be applied to randomly modify the shape of the hull and create chromosomes of new solutions. To demonstrate the effects of different mutation rates, a comparison was carried out using mutation rates from 0.1 to 1.0 in incremental values of 0.1 (505, 510, 515, 520, 525, 530, 535, 540, 545, 550) with a crossover rate of 0 to evaluate the effects of mutation only.

The results obtained are shown in Figure 35. It may be observed that the solutions generally performed better as the mutation rate increases. For example, mutation rates of 0.3 and 0.5 (515, 520, 525) have higher resistance values as compared to mutation rates of 0.7 to 0.9 (535, 540, 545), where solutions with the lowest resistance values were found. This is

expected as the higher the mutation rate, the higher the chances of the solutions being perturbed, leading to more new solutions discovered. However, unlike crossover, most solutions in mutation converged much later, around the 50th generation onwards. This demonstrated that mutation is a useful mechanism to inject more diversity to the solution space. This is very beneficial after the optimisation has been running for some time and the search starts to stagnate.

Fitness Evaluation

To measure the 'fitness' of the parent ships and child ships later, the performance of each hull form design is evaluated based on the objective function. In hull form optimisation, there are many objective functions relating to the shape of hull that may be improved, including resistance, seakeeping, stability, structural strength and cargo capacity. The selection of an objective function varies widely according to the type of ship and design specification prescribed by the ship owner. As an example in hull form optimisation, the objective functions that may be affected by the hull shape (resistance and seakeeping) are considered.

Candidate design solutions may be assessed using semi-empirical methods such as the Holtrop and Mennen method for resistance analysis and strip theory for seakeeping analysis. This is in view of the large number of candidate solutions to be evaluated and these methods can provide fast and good estimations, which are particularly suited for the initial ship design process. Higher fidelity CFD methods such as potential flow or RANS may be applied at later design stages to validate the optimal design.

Referring to Figure 27, after evaluation of each body design in the initial population in block 220, two parent vessels (i.e. a pair of vessels or hull designs) are selected for subsequent reproduction process in block 225. Since the initial population uses designs of existing ships, the random selection of the parents in block 225 may be used. Advantageously, even with a small initial population available in the hull form library, random selection increases the possibilities of combination and the shape variations in the child solutions, thereby increasing the diversity of solution and lead to better designs.

In block 230 the crossover combination may be performed based on a crossover rate, where new hull designs are generated by combining the geometry of two parent vessels using the cross-morph approach. The crossover rate is a probability of the combination occurring. Each pair of parents may produce from a few to hundreds of child solutions by

varying the magnitude of the morphing parameter (*t*) and cross-point location can also vary along the entire length of vessel, except for the extreme ends which may be omitted as explained. For example, in Figure 11(b) and 13(b), a *t* interval of 0.1 is used. By changing the *t* interval to 0.01 or 0.001, *t* of multiple amplitude may be generated and increase the overall shape variation. If the crossover combination fails to occur, the parent solution (design) is carried over to be the child solution. The cross morph combination may be set to generate one or two combined designs ("child" solutions) with two (i.e. a pair of) parent solutions. Selection without replacement of the parents may be done, in which each parent will only be selected once (and randomly combined in cross-over) and all parents will eventually be selected. Advantageously, this allows for the same number of child solutions to be produced, in which the best solutions from all the parent and child solutions are carried over to the next generation and compete again until the best solution emerged at the end.

If more parent solutions are used in the cross morph, more child solutions may be generated with the different possible combinations. In an example, the crossover rate may be set to be at least 0.5, or at least 0.7 (from 0.7 to 1 inclusive of both endpoints), or at least 0.8, or at least 0.9.

In block 235, the initial child solution undergoes mutation using the boundary-morph method based on the mutation rate to produce the final child solution. Thus, 12 child solutions may be obtained as shown in block 240. Fitness evaluation of the child solutions is performed in block 245. The replacement process occurs in block 250 in which the 12 child solutions (block 255) and 12 parent solutions (block 260) undergo non-dominated sorting ranking in block 265. By further using crowding distance sorting in block 270 the 12 best solutions are used to form the next generation population in block 275 while the other 12 solutions are rejected in block 280.

In NSGA-II, replacement may be applied using the elitism approach through front selection followed by distance crowning method and carrying over the fittest individuals into the next generation. The basic principles of non-dominated selection and crowding distance within NSGA-II are provided in Figure 25.

The pseudo code for replacement using distance crowning method from NSGA-II is provided in Figure 32.

Figure 28 shows a method 300 to obtain a new set of body designs for a new vehicle, in particular hull designs. Each step in the method 300 may be performed by one or more processors within a computing system. In block 305, a set of body designs of a vehicle is provided. Each body design is evaluated with respect to at least one objective function in block 310. In block 315, a crossover combination of two or more body designs from the set is performed to provide two or more initial body designs based on a crossover rate. The crossover rate is a probability of the crossover combination occurring, and may be set randomly by the processor, or by a user. The body designs may preferably be selected randomly, in particular when body designs of existing vehicles are used. In an example, the initial body designs may be selected without replacement to allow each body design in the set to be used. In block 320, each of the initial body designs (combined cross morph designs) is provided in a two-dimensional space with a plurality of frame lines. In block 325, two (a first and a second) boundary frame lines are selected in each initial body design. The boundary frame lines may preferably be selected by a user or predefined, and is preferably a non-terminal frame line. In block 330, a reference frame line is selected between the two boundary frame lines, preferably randomly by a processor to avoid bias or by a user. In block 335, a morphing parameter is selected, the morphing parameter is a rate of change between the reference frame line and the boundary frame line/s. The morphing parameter may be selected preferably randomly by the processor to avoid bias or by a user. In block 340, each initial body design is modified based on the morphing parameter and a mutation rate. The mutation rate is a probability of the application of the morphing parameter occurring, and may be selected either randomly by the processor or by a user. If the crossover rate and/or mutation rate is to be randomly selected, a range may be set for the selection to occur in, for example from 0.5 to 1.0, or preferably from 0.7 to 1.0. Preferably, intermediate frame line/s between the reference frame line and boundary frame line may be adjusted based on a modified morphing parameter, wherein the modified morphing parameter is dependent on the morphing parameter of the reference frame line and the location of the intermediate frame line/s with respect to the reference frame line. In block 345, a plurality of new body designs are generated by modifying the initial body design. In block 350, each of the new body designs are evaluated based on the at least one objective function (used in step 310). In block 355, the body designs in the set and the new body designs are ranked, and a new set of body designs are provided (or chosen) based on the ranking in block 360.

<u>Application of MEC to container ship design</u>

To demonstrate the effectiveness of MEC, automated single-objective optimisation was performed on the hull form of a container ship to minimise the total resistance of the vessel. Three case studies were used to assess the effects of different initial population sizes (and variety of vessels) and different crossover and mutation rates on the optimisation performance. In the first case study, a large initial population of 12 vessels of different types was used. In the second case study, the initial population was reduced to four vessels of the same type. In the third case study, the initial population in case study 2 was expanded from four to 12 vessels using constant-morph. The results obtained from MEC were also validated with an existing SBD commercial software to compare the efficiency gain and performance improvement. The results demonstrate that MEC may be employed successfully to automate the hull form design process for different initial population sizes, with an ability to produce optimal solutions for single-objective optimisation, and is suitable for use with designers and manufacturers of varying size.

For the three case studies, 36 different crossover and mutation rates were applied to compare and examine the impact of different crossover and mutation ratings on large and small initial populations. MATLAB was used in the following case studies.

The design specifications for the container ships are as listed below:

<u>Principal Dimensions</u>

Length between perpendicular (LPP)	= 185m
Breadth (B)	= 32m
Draft (T)	= 9m
Speed (V)	= 20 knots
Displacement Volume (Δ)	= ≤ 34,358.7 tonnes

<u>Objective Function and Constraints</u>

The single-objective function was to minimise overall resistance with a given design specification. Displacement volume (metric ton) was set as design constraint so that the ship's cargo capacity was not compromised (reduced) while improving the objective function.

The single-objective optimisation was formulated as follows:

Minimise $f = Rt$

Subject to: LPP = 185m, B = 32m, T = 9m

Δ = ≤ 34,358.7 tonnes

where *Rt* was the total resistance, *LPP* was length between perpendicular, *B* was breadth (moulded), *T* was draft and Δ was the displacement of the ship in tonnes.

Hull Form Library

The principal dimensions of the 12 existing (parent) vessels are provided in Table 2:

Table 2: Principal Dimensions for 12 existing (parent) ships

Ship	**Ship type**	**Length between perpendicular, LPP (m)**	**Breadth (m)**	**Depth (m)**
1	Container ship A	202	32.2	19.1
2	Container ship B	185	32	19.1
3	Container ship C	120	23	11.2
4	Container ship D	145	13.6	13.6
5	Roll-on/ roll-off ship (ROPAX)	210	34	17.1
6	Bulk carrier	220	36	23.75
7	Product tanker	171	31	15.6
8	Chemical tanker	126.5	21.5	10.5
9	Very Large Crude Carrier (VLCC)	314	58	31
10	Pipe-laying ship	242	45	21.1
11	Cable-laying ship	121	23	12.5
12	Offshore accommodation ship	168	24	13

These 12 vessels are proven designs that are ‘hand-crafted’ by experienced designers and used as parents in the initial population. Wire-mesh diagrams and body plans for the 12 existing (parent) vessels are shown in Figures 36A/B and 37A/B respectively.

Case Study 1: Large Initial Population

In the first case study, 12 existing vessels in the Hull Form Library were set as the initial population. As above low crossover and mutation rates may not yield good designs. Hence, different crossover and mutation rates between ranges of 0.5 to 1 were investigated to select the optimal settings. A total of 36 different combinations were assessed.

A summary of the initial settings used is provided as follows.

- Initial populations = 12 vessels
- Crossover rates = 0.5 to 1.0
- Mutation rates = 0.5 to 1.0
- Total generations = 100

Based on the design criteria, the initial hull forms were first evaluated using the Holtrop method to estimate the total resistance, *Rt*. Subsequently, the hull shapes were modified using single-point cross-morph and boundary-morph. The new design solutions were then carried over to the next generation, where the entire process is repeated for 100 generations. Hull forms from the first generation are shown in Figure 38 to illustrate the geometric changes after cross-morph and boundary-morph.

Figure 38 shows the hull forms of two initial parent vessels and the geometric changes in the child vessel produced following cross-morph and boundary morph. Figures 38(a) and 38(b) show the parent vessels that were randomly selected from the initial population. These vessels were merged together using cross-morph, at a random point resulting in child 1, as shown in Figure 38(c). It may be seen that the mid body section modified by cross-morph (transition section) provides a smooth transition between the two parent vessels but retains a longer portion of ship 1 aft body and shorter portion of ship 4 forward body (in blue).

Using boundary-morph, child 1 was mutated into child 1’ as shown in Figure 38(d). It may be seen that child 1’ has a longer modified mid body that extends into the forward and aft body of the two parent vessels using boundary-morph. The result is a new hull body, which had been modified extensively, leaving only a small portion of forward and aft body that is the same as the two parent vessels. It may be seen the shape of child 1’ has a slightly slender forward body and fuller mid-body as the displacement volume was ‘shifted’ towards the aft body of the vessel. By doing so, it enables the shape of the forward body to be more

streamlined, thereby reducing the resistance and at same time maintain the minimum displacement.

A total of 36 simulations were performed using different combinations of crossover and mutation rates. The convergence charts shown in Figures 5.4(a) to (f) present the results obtained. In each figure, the crossover rate is kept constant and the mutation rate varies from 0.5 to 1 (incremental values of 0.1). The crossover rate of Figures 5.4(a) to (f) increases from 0.5 to 1 with incremental intervals of 0.1.

Several key observations may be made from Figure 39. First, it is observed for crossover rates of 0.5 and 0.6, very high mutation rates were required to prevent premature convergence and poor performance. For instance, from Figures 39(a) (Cross 0.5, Mut 1) and 5.4(b) (Cross 0.6, Mut 1), a mutation rate of 1 was needed to compensate for the low crossover probabilities (0.5 and 0.6). This was likely due to the initial population having a limited number of parent vessels available for crossover. Thus the parent pairs selected for crossover were very similar or identical, leading to the child solutions having very similar or even cloned characteristics and performances. This coupled with a low crossover rate may result in solutions found being “stuck” in a local optima, resulting in premature convergence as the optimisation progresses. In most applications of GA, the range of the initial population typically falls in the region of high two-digits or even hundreds. However, the number of existing hull forms is limited and difficult to obtain, making GA an unconventional choice for hull optimisation with a small initial population. Existing methods of hull optimisation using GA require the user to provide a wide range of parameters (for example length. breadth, height, block coefficient, prismatic coefficient, length/breadth ratio etc.) to create a large initial population. An example of GA application is where the user defines a set of new geometry parameters from an existing vessel by adjusting the length, breadth, and height to create an additional or new set of designs to form the initial population. In contrast, the present method uses the existing hull forms available in the digital hull form library, thus removing the need for the user to create additional hull designs to form the initial population.

Mutation, on the other hand, provided the more “bespoke” modifications where only small sections of the hull form are modified at a time. More importantly, it has a greater number of degrees of freedom. During mutation, sections of the hull might be modified in any direction. This is a key difference as crossover only morphs the hull forms in the x direction. From Figures 39(a) and (b), it may be seen that with the exception of mutation rates of 0.9 and 1, the process started to converge very quickly around the 20th generation for all other

settings. Furthermore, the solutions found with higher mutation rates were also more superior.

For traditional optimisation, where the population size is larger (hundreds of individuals), a high crossover rate coupled with a low mutation rate may provide good convergence. In this case, the initial population is comparatively smaller and hence requires a higher mutation rate to increase shape variation. This may be seen from Figures 39(d) to (f), where crossover rates are 0.8 to 1.0, respectively and the mutation rate is 0.5 so that the search converges prematurely. Nonetheless, it is important to maintain a balance between crossover and mutation rates.

When a high crossover rate was used in conjunction with high mutation rate, the solutions found tended to be sub-optimal. This phenomenon is best observed in Figures 39(c) to (f) where the optimisation performance began to degrade when the mutation rates were increased from 0.7 to 1 for crossover rates of 0.7 and higher. For example, in Figure 39(e) for crossover rate of 0.9 and mutation rate of 1 (Cross 0.9, Mut 1), the optimisation stagnated at around the 10th generation and although the best solution found had better resistance performance (930 kN) compared to the best initial parent (944.6 kN), it was sub-optimal. It is likely that this might have resulted from reasonably good chromosomes which were obtained after crossover were over-perturbed at mutation and as a consequence, became too fragmented and lost its structure. This means that a good chromosome might not survive the current generation and be carried forward to the next as the optimisation progressed, resulting in only sub-optimal solutions found at the end of the optimisation. In hull form design, this may be thought of as over-refinement of the geometry of the hull resulting in irregular and infeasible forms. Typically, both crossover and mutation should encourage construction of new solutions, however, this could prove counter-productive when overused. Balancing this “construction-destruction” paradox is important to the success of MEC. For Case Study 1, the optimum crossover and mutation rate was determined to be 0.8 and 0.7 respectively. The solution space for this setting (Cross 0.8, Mut 0.7) is shown in Figure 40.

From Figure 40, it may be seen that the solution space is divided broadly into 3 regions. The first (top right corner) covered the solutions from the initial population. The second region mainly comprised of solutions found in the first 10 generations and the third region located at the bottom left corner of the plot is made up of solutions starting from around generations 11 to 100. From the left downward shift of the solution distribution and the

distance between the three regions, it may be deduced that better solutions were found very quickly (within the first 10 generations of the optimisation) and the search began slowing down beyond that with solutions having only incremental performance improvements. This characteristic is not uncommon in optimisation problems with limited individuals in the initial population which may sometimes be thought of as having converged prematurely. Nonetheless, as explained earlier, mutation might have resulted in a slightly more diverse pool of individuals which were carried forward to the next generation for reproduction. As a consequence, incremental improvements were observed. The performance of the best initial parent and the six unique solutions found at the end of the optimisation are shown in Table 3. It may be seen that all solutions were within the displacement constraint, of which three solutions had better resistance performances than the best parent design (Container Ship A, 944.6 kN) and the optimal solution (Solution 1189, 839.32 kN) having an improvement of 11.14%.

Table 3: Best initial parent and child solutions optimising resistance function (high initial population)

Solution	**Resistance (kN)**	**% improvement over best initial parent**	**Displacement (tonnes)**
Best initial parent-Ship no. 1 (Container Ship A)	944.60	**-**	32,365.2
Solution 1189	839.32	11.14	34,460.16
Solution 1191	840.08	11.06	34,401.87
Solution 1199	852.05	9.79	34,821.34
Solution 1190	946.91	-0.24	34,416.65
Solution 1198	947.01	-0.25	34,360.05

Solution 1200	949.16	-0.48	34,435.97

The wire-mesh diagrams of the best child solutions from the (a) 1st, (b) 5th, (c) 10th, (d) 20th, (e) 50th and (f) 100th generations are presented in Figure 41 and show the evolution of the best solution as the optimisation progressed. At the start of the optimisation, parent ship 2 (Container Ship B) in the initial population was carried forward into the first generation. The wire mesh diagram of the hull is shown in Figure 41(a). Figure 41(b) shows the hull form obtained in generation 5 after parent ship 2 was cross-morphed with the aft body section of initial parent ship 9 (VLCC). The effect of this new combination is the volume displacement at the aft body was reduced significantly, which is not ideal where cargo capacity is concerned. As the optimisation progressed, a new aft section which resembled initial parent ship 4 (Container Ship D) was introduced in generation 10 during crossover and the bow area was modified in boundary-morph. This new combination provided more displacement volume at the aft section and created more cargo spaces. The resultant hull form is shown in Figure 41(c). It may be seen from Figures 41(d) to 41(f) that between the 20th to 100th generations, the bow body began to narrow and the mid body of the vessel started to expand. This may be a direct effect of boundary-morph which bodes well with the distribution shown in Figure 40 where performance improvements from generation 20 onwards were mainly driven by mutation.

The body plans of the best initial parent (ship 1- Container Ship A) and best solution (Solution 1189) are shown in Figure 42.

It may be observed from Figure 42 that the hull lines from the best child are relatively smooth (without broken lines or bumps) and mostly feasible. This is a considerable achievement given that the hull form underwent approximately 1200 (100 generations with 12 parent solutions in initial population) rounds of modifications. Comparing the two hull forms of the best solution and the best initial parent, it is clear that they are completely different. For example, it may be seen that the aft body of the best solution has taken on the shape of the initial parent (ship 7 – product tanker) while the forward body resembles that of the initial parent (ship 9 - VLCC). This is good illustration of how crossover and mutation has worked together to produce a highly feasible hull form that meets the design specifications.

The results show that MEC has 'intelligently' sized the shape of the vessel to meet the design specifications. The optimisation was performed automatically without any input from the designer beyond the initial settings prior to the start of the process.

Case Study 2: Small Initial Populations (Four Vessels)

In the second case study, only four container ships from the Hull Form Library were used as parent vessels in the initial population. As with Case Study 1, 36 combinations of crossover and mutation rates (ranging from 0.5 to 1.0) were applied and the results are presented in Figure 43.

The settings used for the optimisation are shown below:

- Initial populations = 4 vessels
- Crossover rates = 0.5 to 1.0
- Mutation rates = 0.5 to 1.0
- Number of generations = 100

From Figure 43, a number of interesting observations may be made about the optimisation. Some exhibited similar trends to those observed in Figure 39 for Case Study 1 while others did not.

First, for crossover rates 0.7 and below, high mutation rates were required to improve the performance of the search. For example, in Figure 43(a) where the crossover rate was 0.5, better solutions were found as the mutation rate increased. This is most clearly observed for mutation rates from 0.5 to 0.7 and bodes well with the findings from the first case study. However, unlike Case Study 1 where sub-optimal results were obtained when both the crossover and high mutation rates were increased above 0.7 (Figures 43(c) to 43(f)), improvements in performance were observed in this case study as the crossover and mutation rates continued to increase. This is evident from Figures 43(c) to 43(f) that better solutions were found for crossover and mutation rates of 0.7 to 1. In almost all cases, the best solution was obtained when the mutation rate was 1. This may be attributed to the lack of new shapes created during crossover due to low initial population and high mutation in this case provided the much needed shape variations to improve the performance.

Second, as with Case Study 1, a high mutation rate was needed to prevent premature convergence. For example, from Figures 43(c) and (d), it may be seen that for crossover rates of 0.7 and 0.8, performance improvements were found very early on in the

optimisation, however this tended to plateau around the 20th generation and little or no improvement was made beyond this point.

Case studies 1 and 2 show that crossover on its own provide limited improvement to the solutions, especially as the optimisation progressed over a number of generations. This observation particularly resonates with the second case study when the initial population was small with very similar structures. To support this observation, another simulation was carried out by setting the mutation rate to 0 and crossover rate ranging from 0.5 to 1.0. The result of this simulation is provided in Figure 44.

Figure 44 shows the effect of different crossover rates when mutation was set at 0. There were two distinct outcomes. The resistance was observed to be lowest (close to 1000 kN) when the crossover rate was at 0.5 and the higher rate of 0.9 and 1.0 (the extreme ends). Crossover rates of 0.6 to 0.8 had a higher resistance of 1050 kN (i.e. worst outcome). Compared to Figure 43 where mutation rate was at a range of 0.5 to 1.0, the overall (averaged) resistance had worsened by about 9.7% in this case without mutation. This demonstrated the role and importance of mutation to create new hull shapes with better improvement.

The solution space for a crossover rate of 0.7 and a mutation rate of 1.0 (Cross 0.7, Mut 1.0) of Case Study 2 is shown in Figure 45. Similar to Case Study 1, three distinct regions were identified. The first region, located to the right of the plot, contains solutions from the initial population and first 10 generations of the optimisation. The second region contains solutions from generations 11 to 30 and the third region contains solutions from generations 31 to 100. As with Case Study 1, the “movement” of solutions in the search space tended toward a left downward shift, an indication of convergence as the optimisation progressed. Nonetheless, when one considers the rate of this shift, it becomes apparent that this was slower compared to Case Study 1. In Case Study 1, the optimisation progressed very quickly toward the optimal solution space (Region 3) where solutions found were crowded around the optimal solution within the first 10 generations. However, in Case Study 2, it took another 10 generations before the search started to converge towards Region 3. This might be due to the smaller number (and type) of parent vessels in the initial population as compared to Case Study 1. This limited the options available for crossover and mutation and further affirmed the need for higher mutation rate in this case.

Table 4: Best initial parent and child solutions for resistance optimisation using a small initial population

Solution	**Resistance (kN)**	**% improvement over best parent**	**Displacement (tonnes)**
Best initial parent-Ship no 1 (Container Ship A)	944.60	**-**	32,365.2
Solution 397	876.31	7.22	34,412.99
Solution 398	876.99	7.15	34,365.52
Solution 399	877.74	7.07	34,368.46
Solution 400	878.83	6.96	34,458.39

Table 4 shows the best initial parent and child solutions for Case Study 2. The optimal solution (Solution 397) has a resistance of 876.31 kN, an improvement of 7.22% over the best parent (ship 1). The hulls of the best child solutions from the 1st, 5th, 10th, 20th, 50th and 100th generation are presented in Figure 47.

Figure 47 shows the shape changes to the solutions during the optimisation. It may be observed that the crossover combination was very similar to each other during 1st – 5th generation as seen in Figures 47(a) and 47(b). This may be because there were only four vessels of the same type in the initial population. Despite the similarity, the resemblance of the initial child solution to the forward of initial parent ship 2 (Container Ship B) and aft of initial parent ship 3 (Container ship C) may be observed. This new combination created during crossover did not vary greatly from the original parent designs and hence did not provide significant improvement to the performance. However, from the 10th generation as shown in Figure 47(c) onwards, it may be observed that the mutation concurrently reduced the bow section and increased the mid-section body until the 100th generation in Figure 47(f). This created significant shape changes especially to the forward and aft body of the new child solution compared to the initial parents. It may be observed from Figure 47(f) that the bow of the final child solution was very ‘sharp’ and streamlined, which helped to reduce the overall resistance of the vessel. This is consistent with the previous case study, and demonstrates the ability of the described method to modify the hull, resulting in a hull with

a narrow bow, fuller mid-body and lower resistance. The body plan of the best child (Solution 397) and best initial parent (ship 1 – Container Ship A) are plotted in Figure 46.

From Figure 46, it may be seen that although there were changes in both the forward and aft sections of the ship, some attributes of the initial parent (ship 1 – Container Ship A) were retained. For example, the aft section of the best child (Solution 397) was similar to that of the initial parent (ship 4 – Container Ship D) and the forward section of the initial parent (ship 2 – Container Ship B). Similar to Case Study 1, the bow section had been extensively modified during boundary-morph, resulting in a very slender bow which helped to reduce the resistance. All modified lines were smooth and the solution feasible. This result demonstrates that MEC is well-suited for optimisation problems where there are only a small number of individuals available in the initial population.

Case Study 3: Expansion from Small to Large Initial Population

In this case study, the same initial population from Case Study 2 was used. However, eight new vessels were created using constant-morph and added to the initial four to form an initial population of 12 vessels. This process is illustrated in Figure 48.

In Figure 48, the frames of the source and target vessels are on the left and right while the frames of the child solutions created through constant-morph are in the middle. It may be seen that the hull forms of the child vessels are highly streamlined and have large deck spaces. This is an important requirement for a container vessel where lower resistance and higher payload are both highly desirable properties. This is a very efficient way to rapidly increase the size of the initial population. Similarly, 36 combinations of cross-over and mutation rates ranging from 0.5 to 1.0 were applied to select the optimum settings for this case study. The MEC settings are summarised below.

- Initial populations = 12 vessels
- Crossover rates = 0.5 to 1.0
- Mutation rates = 0.5 to 1.0
- Number of generations = 100

The convergence charts are shown in Figure 49. By comparing the convergence plots between Case Studies 2 and 3, two key observations may be made. First, as seen in Figure 49, most of the convergence took place after 50-60th generation as opposed to 20-30th generation in Case Study 2. The overall resistance was also improved from around 880 kN to around 850 kN for the best child solution. This demonstrated that by increasing the initial

population from 4 to 12 vessels using constant-morph, it helped to increase the shape variations and diversity of solutions, which led to delayed convergence and better performances.

Second, higher crossover rates were observed to result in better performances in the expanded initial population in Case Study 3 compared to the smaller initial population in Case Study 2. For example, when crossover rate was increased from 0.5 to 1.0 with the mutation rate set at 0.8, there was no improvement observed. In this case study, the resistance reduced by -4.7% as crossover rate increased from 0.5 to 1.0 for the same mutation rate. This difference might be attributed to a better crossover effect where more diverse solutions were created by combining a larger variety of parents from the increased initial population.

The solution space for the most optimal setting (Cross 1.0, Mut 0.8) is shown in Figure 50 and shows that the solutions found in Case Study 3 tended to be more spread out across the entire solution space compared to Case Studies 1 and 2. There may be a few reasons for this. First, there are no distinct regions which demonstrate there are neither any local optima nor traps found in the solution. Second, the expanded initial population had more diverse individuals (compared to Case Study 2). This demonstrates the efficiency of constant-morph to create more new initial parents to form into a larger initial population. These in turn resulted in a wider coverage of the search space and increased the likelihood of better solutions being discovered during the optimisation.

It may be observed from Figure 50 that the increase in diversity might be likely attributed to the additions of new initial population's solutions (indicated as Initial') that are created through constant-morph, which are distributed evenly between the initial parents (indicated as Initial). For example, initial' parent (Child S1-S3) was positioned between initial parents ship 1 and ship 3 and this is similar to initial' parent (Child S1-S4) that was located between ship 1 and ship 4 in the solution space. Due to the similarity of these new initial' solutions with existing initial parents, this may also explain the reason for the well spread solutions over the generations. The performance of the best parent and 12 best solutions in the final generation are presented in Table 5.

Table 5: Best parent and the solutions found at the end of the optimisation ranked in order of performance.

Solution	**Resistance (kN)**	**% improvement over best parent**	**Displacement (tonnes)**
Best Parent- Ship 1	944.60	-	32,365.2
Solution 1189	844.86	10.55	34,384.72
Solution 1193	848.11	10.21	34,406.61
Solution 1195	848.50	10.17	34,426.19
Solution 1199	848.52	10.17	34,426.33
Solution 1190	931.38	1.39	34,401.73
Solution 1191	931.70	1.36	34,479.34
Solution 1192	931.93	1.34	34,486.79
Solution 1194	932.48	1.28	34,477.61
Solution 1196	932.61	1.26	34,487.38
Solution 1197	933.14	1.21	34,607.14
Solution 1198	934.04	1.11	34,601.83
Solution 1200	934.50	1.06	34,627.16

The best solution (Solution 1189) achieved a resistance of 844.86 kN, an improvement of 10.55% over the best parent design. In comparison to Case Study 2, there was an improvement of 3.33%. This improvement further affirmed the importance of having diverse solutions in the initial population and the effectiveness of constant-morph to expand the initial population very rapidly. The hull forms of the best solution taken from the (a) 1st, (b) 5th, (c) 10th, (d) 20th, (e) 50th and (f) 100th generations are presented in Figure 52.

It may be seen in Figure 52(a) that the 1st generation started off with a solution that is similar to the initial parent (ship 1). Following which, crossover resulted in a new combination as shown in Figure 52(b) in the 5th generation of a bow body of the initial parent (ship 2) and an aft body of the expanded initial' parent (child S2-S4-0.8). This new combination continued to be carried over to the subsequent generations while the entire

section of the hull form was continuously ‘fine-tuned’ until the 100th generation through mutation. Similar to the other two case studies, it may be observed from Figure 52(f) that the final shape of the best child at 100th generation has a very fine and narrow forward body, which helps in reducing the overall resistance. The mid to aft body of the hull is also observed to be much fuller as compared to the solution from the 50th generation as shown in Figure 52(e). These modifications compensated for the loss of volume at the bow by shifting it to the aft body in order to maintain the minimum displacement. The body plans of the best child (Solution 1189) and best initial parent (ship 1) are plotted in Figure 51.

Similar to previous case studies, the best child solution and best parent have rather distinct hull forms. Figure 51 shows that the aft section was similar to child S2-S4 (t = 0.8), which was created using constant-morph while the forward section took the shape of the initial parent (ship 2). Compared to the best parent (ship 1), the cross-section area at the aft area of best child solution expanded largely due to the shifting of displacement volume from the forward section to the aft of the vessel. At the same time, it may be observed that the bow section shrank considerably to create a slimmer cross section thereby reducing the overall resistance. More importantly, the hull lines of the best child solution are still highly smooth and feasible.

<u>Validation of Solutions from MEC with NAPA</u>

In this section, the solutions created by MEC were validated against commercial NAPA ship design software (NAPA). NAPA provides highly customised manager functions where the user may apply hull form optimisation. These manager functions include geometric transformation using FFD, optimisation using Multi-Objective Genetic Algorithm (MOGA) P. Barberio-Corsetti, “Technical Assistance for Genetic Optimization of Trellis Codes,” Final report for the Communications System Section (XRF) of ESTEC, Eurospacetech Frequency, vol. 94 no. 02, 1996, and resistance evaluation using the Rankine-source panel method Y. Tahara, “A Numerical Approach for Steady Ship-Wave Problem Based on Dawson-Type Rankine-Source Method with Non-H-Type-Topology Free-Surface Panels,” J. Kansai Society of Naval Architects, no. 230, pp. 147-152, 1998. An experienced designer was tasked with optimising the hull form of a container ship based on the same design specification. The designs were assessed based on the overall time taken and improvement achieved with MEC. The steps and results of the validation are provided below.

Step 1 - 3D Surface Modelling

Firstly, the hull form was created manually in NAPA. As a starting point, an existing vessel in the initial population was used. This is one of the most time-consuming processes where the 2D offset data was imported using the offset manager function into NAPA and then modelled and faired to ensure that the surfaces are fully intact. The final surface of the initial hull is shown in Figure 53.

Step 2 - Geometry Modification

In the optimisation function, the hull form was modified using FFD by extending the bulbous bow further forward. Firstly, a bounding box around bulbous bow was created by the designer. Then, three movement points were set: 5m towards +X direction, 3m towards +Z direction and 2m towards -Z direction. The outcome of the geometry transformation is shown in Figure 54.

Step 3 - Panelisation Of Hull Surface

To evaluate the resistance of the hull, the model was first panelised using 1960 hull panels and 1000 free surface panels are selected for evaluating the fluid region as shown in Figure 55. Potential flow was then used to estimate the flow field around the ship hull.

Step 4 - Optimisation and CFD Evaluation

Optimisation was carried out using the GA features provided in NAPA with the following settings. For comparison, these settings were set close to those used in the MEC methods described above. A higher crossover setting was applied to increase shape variations as mutation in NAPA is more localised using Free-form Deformation (FFD), when compared to global transformation of the entire hull using MEC. In this case, only the bulbous bow was mutated in NAPA, as modifying the entire hull form using FFD would be too disruptive to the hull shape, due to the limited number of control points available. The results of the optimisation are provided in Table 6.

Number of individuals in a population	= 10
Number of generations	= 100
Mutation probability	= 0.5
Crossover probability	= 1.0

Table 6: Optimisation results comparing initial vessel and best five child designs

Solution ID	**Blend 1**	**Pressure resistance coefficient (CPRS)**	**Improvement from initial design (%)**
Initial	0	0.254	-
103	8.2795	0.252	0.79
96	**9.5307**	**0.25**	**1.6**
160	8.8022	0.253	0.39
199	9.6480	0.251	1.19
82	9.8045	0.252	0.79

Table 6 shows the optimisation results, and an improvement of 1.6% was obtained from the best solution (ID 96). The wave profile of ID 96 is shown in Figure 56.

The breakdown of tasks and the time taken from start to finish for one simulation using NAPA and MEC are compared in Table 7.

Table 7: Task breakdown and time taken for each simulation in NAPA and MEC

Step	**Task**	**NAPA Time (hours)**	**MEC Time (hours)**
1	3D Hull form creation from offset table	17.6	0
2	Setting up free-form deformation manager function	0.5	0
3	Setting up Panelisation manager function	10	0
4	Setting up optimisation manger function	1.5	0
5	Setting up CFD analysis	1	0
6	MOGA optimisation	1.5	0.1
7	Extraction of results	0.5	0

	Total time taken	**33.1**	**0.002 (10 sec)**

Comparison of Results between MEC and NAPA

Table 8 presents the results using MEC (from Case Study 1) compared to that from NAPA in terms of both the performance and time taken to complete the optimisation.

Table 8: Comparison of time taken and optimisation result between existing SBD tool and MEC

Criteria	**MEC (Case study 1)**	**Existing SBD (NAPA)**	**Differences (MEC – NAPA)**
Total time taken	10 sec x 36 combinations = 360 seconds (6 minutes)	33.1 hours	33 hours
Improvement in resistance compared to initial design	11.14%	1.6%	9.44%
Number of design solutions evaluated	1200 x 36 combinations = 43,200	1000	42,700

In both aspects, it is clear that MEC had better performances over NAPA. Two key benefits are noteworthy. First, it was able to efficiently navigate the design space within a short period of time. It took 10 seconds to run through 1200 design solutions (6 minutes with 36 combinations) whereas NAPA took 33.1 hours for 1000 solutions. As shown from Table 7, the real time savings was primarily due to the additional step for 3D surface modelling used in NAPA. The MEC method provides significant savings in the computation time required. As it uses only 2D curves, the need to convert the 2D offset data into 3D surface for the performance evaluation is removed and hence the overall time taken is significantly reduced.

Second, through its unique morphing schemes, it was able to mix-and-match and modify existing solutions to create newer solutions automatically. These features are extremely useful as designers may now use MEC to carry out the initial optimisation for a design problem. This frees up time for them to focus on more important tasks which may otherwise not be afforded.

To demonstrate the complete design loop from the 3D CAD surface to discretised 2D offset data and vice-versa, the input data of the initial parent designs can also start from 3D CAD surfaces and convert to 2D offset points using hull-to-offset manager function in NAPA. The initial vessel model (container ship A) is in a 3D CAD format based on NURBS patch surfaces in NAPA. This surface is then discretised from 3D into 2D offset points using the hull-to-offset manager function in NAPA. The final output is a 2D representation of the same vessel in offset data format that is ready to be included in the hull form library for automatic HFDO using MEC. In a similar fashion, after completion of the HFDO process, the optimised hull form (from case study 1) which is in 2D offset format may also be converted back to 3D CAD format using the offset manager function in NAPA. By converting the optimised hull form back into 3D CAD format, it allows the 3D model to be validated using CFD.

To further demonstrate the usability of the 2D offset curve format, vessel geometries were compared with the 3D CAD surface (from the optimised child vessel in case study 1). The results are shown in Table 9.

Table 9: Comparison of vessel geometries, hydrostatics and performance of the optimised child vessel (solution 1189) for the 2D offset curve and 3D CAD surface format

Parameters	**2D offset curve**	**3D CAD surface**
Vessel model	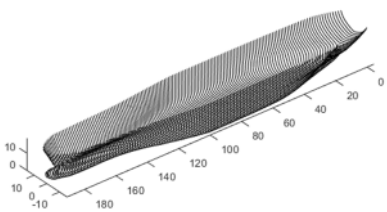	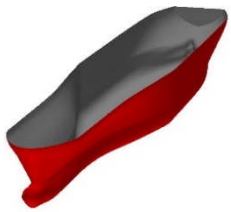
Principle dimensions (m)	185(Lpp) x 32(Breath) x 9 (Draught)	185(Lpp) x 32(Breath) x 9 (Draught)
Displacement (tonnes)	34460.16	33903.3

Block coefficient, Cb	0.631	0.619
Prismatic coefficient, Cp	0.644	0.638
Waterplane area coefficient, Cw	0.673	0.683
Total resistance (kW)	839.328	1028.745

Here, differences between the two vessels in terms of displacement (556.69 tonnes) and total resistance (189.417 kN) were observed. The discrepancy in displacement may be attributed to the additional volume that arises from the spacing between the transverse frames for the 2D offset curve calculations. This may be resolved by reducing the frame spacing of the offset table to the smallest value possible by creation of new transverse frames. The disadvantage is that more 2D offset points are created which increases the computation time. The difference in the total resistance may be due to two reasons. The empirical method (Holtrop & Mennon) applied for calculating the total resistance of the 2D offset model was deployed using historical data from conventional vessels. Hence, the resistance is very close to the data for the original vessel container ship A. However, the optimised child vessel may be significantly different to the parent, following crossover and mutation in the method described above. This could result in discrepancies in the results. Therefore, the potential flow method used to calculate the total resistance of the 3D CAD surface model appears to be more accurate and of higher value, when compared to the 2D offset curve model. Secondly, some geometric details may not be accurately captured in the 2D offset model, when compared to the 3D CAD surface model. To further improve the accuracy, more detailed CFD analyses such as potential flow or RANS, may be used in place of the empirical method.

For completeness, a detailed time-cost analysis of the complete-loop comparing the start of the optimisation using the 2D offset curve and the 3D CAD surface model are provided in Table 10. The conversion from 3D to 2D adds approximately one hour to the optimisation

Table 10: Comparison of vessel geometries, hydrostatics and performance of optimised vessel (solution 1189) for the 2D offset curve and 3D CAD surface format

Task	**2D offset curve**	**3D CAD surface**	**Level of automation**
Convert from 3D CAD surface to 2D offset curve format	-	1 hour	Semi-automatic
Optimisation process using MEC	0.1 hours	0.1 hours	Fully automatic
Convert 2D offset curve to 3D CAD surface	17.6 hours	17.6 hours	Semi-automatic
Total time (hours)	17.7 hours	18.7 hours	

The combined results for the three case studies are summarised in Table 11.

Table 11: Summary of MEC Optimisation Results

Parameters	**Case study 1- large initial population**	**Case study 2- small initial population**	**Case study 3- expanded initial population**
MEC settings and constraints			
Initial population	12	4	12
Optimal crossover rate	0.8	0.7	1.0
Optimal mutation rate	0.7	1.0	0.8
Generations	100	100	100
Principal dimensions (m)	185 (LPP) x 32 (Breadth) x 9 (T)		
Minimum displacement volume (tonnes)	34,358.7		
Best initial parent- Ship 1 (Container Ship A)			
Displacement (tonnes)	32,365.2		
Resistance (kN)	944.6		
Best child solutions			
Displacement (tonnes)	34,460.16	34,412.99	34,384.72

Resistance (kN)	839.32	876.31	844.86
% improvement over best initial parent	11.14	7.22	10.55
Time taken for 36 runs (minutes)	6	6	6

Four key conclusions may be drawn from the three case studies. First, comparing high and low initial populations (Case Studies 1 and 2), it may be concluded that higher initial populations resulted in more diverse child designs and hence, better improvements. This is demonstrated as the overall improvement decreased from 11.14% to 7.22% when the initial population was reduced from 12 vessels in Case Study 1 to four vessels in Case Study 2. Furthermore, the type of vessels in Case Study 1 were more varied as compared to Case Study 2 where all vessels were of the same type.

Second, it was proven that MEC yielded better designs even for very low initial populations. Expanding the initial population to 12 vessels using constant-morph enabled very low initial populations to increase their diversity, enabling more shape variations to be created and thereby increasing the performance improvement from 7.22% in Case Study 2 to 10.55% improvement in Case Study 3. This same concept may be applied to hull form libraries with limited sizes to rapidly increase their initial population and lead to better diversity and convergence.

Third, comparing Case Studies 1 and 3 suggested that more diverse ship types could potentially produce more shape variations and result in better (performance) solutions, though the improvement was marginal (11.14% for a mixture of vessels and 10.55% for all container ships).

Finally, it may be concluded that crossover and mutation played important roles in influencing the outcome of solutions generated by MEC. Comparing the convergence charts obtained from the three case studies, the optimal crossover and mutation settings varied in the range from 0.7 to 1.0. As demonstrated in the results, the optimal setting depended greatly on the size of the initial population and also the ship types available in the Hull Form Library. In the scenario of high initial population - high mix (vessel types) performed in Case Study 1, high crossover and mutation settings (0.7 - 0.8) were required to prevent pre-matured convergence to the optimisation process. Conversely, very high

crossover and mutation settings (e.g. 1.0) resulted in sub-optimal solutions due to over-perturbation. For a low initial population – low mix scenario done in Case Study 2, high crossover (0.7) and very high mutation (1.0) were required to produce the most optimal solutions. This may be because crossover was not able to generate sufficient new shape combination due to the small initial population and mutation rate needs to be increased to produce the much needed shape variations. Case Study 3 is for a high initial population – low mix scenario, in which best results were achieved by increasing the crossover rate to very high (1.0) and mutation rate at high (0.8). This might be attributed to the effect of having more homogenous (similar) initial parents that was achieved through constant-morph, where more diverse solution might have been created by combining different parents from a larger initial population pool using cross-morph, although they might be all of the same vessel types.

The benchmark case demonstrated that the total time taken may be reduced by more than 33 hours while the performance (resistance) may be improved by 9.44% when comparing MEC and the existing SBD tool. However, it should be noted that the results obtained from this study is neither a direct comparison nor conclusive. This is due to reason that both tools used different methods for geometry modification, optimisation and performance evaluation. FFD was used in NAPA to modify only the bow region (localised modification) while MEC used 2D curve morphing to modify the entire hull form (global modification). NAPA used GA for optimisation while MEC used NSGA-II, although both methods are quite similar. NAPA used low fidelity CFD method- potential flow for performance evaluation, which is more accurate as compared to Holtrop method applied in MEC. Nevertheless, the results demonstrated that a fully automated tool such as MEC may be applied effectively to reduce overall time and achieve better performance for hull form design optimisation as compared to existing SBD tools, which are semi-automated.

Some of the achievements from these case studies include, the improvement gained is quite significant (7.22% reduction in resistance in Case Study 2 to 11.14% reduction in Case Study 1) considering that there were no changes to the main dimensions and that minimum displacement was maintained. In most HFDO, the main dimensions and minimum displacements were adjusted in order to allow some ‘room’ for designers to explore. More notably, the original hull used in this case study was an optimised hull form which had already been proven in real applications, and should technically be difficult to further optimise.

Second, the results show that lower resistances are obtainable (with higher displacements) compared to the best parent designs (which have much lower displacements). This is a significant achievement because MEC has made it possible to automatically adjust the hull form to reduce the resistance while simultaneously maintaining minimum displacement. In actual practice, it would be very difficult for a designer to achieve similar results using the manual 'trial and error' approach or conventional SBD approaches, where reducing the resistance would almost always result in reducing the overall displacement.

Third, the geometry of the final modified hull form (or child design) remains relatively smooth with no bumps or steps observed despite undergoing hundreds of rounds of iterations and modifications. This is a unique feature of the 2D curve morphing applied in the methods herein.

Finally, these three case studies demonstrated the versatility and ability of MEC to automatically transform the shape of the hull while simultaneously yielding better and feasible designs for a single-objective optimisation of container ships.

Case Studies 4 and 5 were done on the design of an offshore cable-laying ship. In offshore cable-laying operations, it is critically important to have a hull with good seakeeping characteristics as they determine the 'up-time' the vessel can safely operate. Seakeeping motions, namely, pitch, roll and heave, are therefore important design considerations for offshore vessels. Another important design objective is the resistance of the vessel. It is expected that the hull should be streamlined to reduce the overall drag acting on the vessel, leading to lower fuel costs. These design criteria are used in the automated multi-objective optimisation of an offshore cable-laying ship.

Objective and Design Specifications

There is no common standard in measuring seakeeping performance but it may be affected by aspects such as ship motions, accelerations, course-keeping and local sea load. Depending on the operation model and travel route, the design criteria varies largely for different types of ships. Three degree of motions, namely pitch, heave and roll were considered in Case Studies 4 and 5 as they are the important seakeeping considerations for design of offshore vessel such as cable-laying ship. In multi-objective optimisation, objective functions may be classified into two main types: non-conflicting and conflicting. For non-conflicting objective functions, objectives work in tandem with one another such that improving one objective results in the improvement of the other objective(s). In contrast,

for conflicting objective functions, improving one objective would result in worsening the performance of the other objective(s). The two case studies evaluated the performance of MEC in handling both non-conflicting and conflicting objective optimisation.

In Case Study 4, the goal was to minimise the heave and resistance of the vessel and demonstrated the performance of MEC for non-conflicting multi-objective optimisation. In Case Study 5, roll and pitch motions were added to further ascertain that the proposed methodology was capable of carrying out both non-conflicting and conflicting objective optimisation.

The design specifications for the offshore cable-laying ship are given below.

Principal dimensions

Length between perpendicular (*LPP*)	= 121m
Beam (*B*)	= 23m
Draft (*T*)	=7.5m
Design speed (*V*)	= 14.5 knots
Displacement (Δ)	≤ 15,000 tonnes

Objective functions and constraints

The multi-objective optimisation was formulated as:

Minimise *f* = *Rt and heave* (Case Study 4)

f = *Rt, pitch, roll and heave* (Case Study 5)

Subject to: *LPP* = 121m, *B* = 23m, *T* = 7.5m

Δ = ≤ 15,000 tonnes

where *LPP* represented length between the perpendicular, *B* was the breadth (moulded), *T* was the draft, *Rt* was the total resistance and Δ represented the displacement of the ship in metric ton (tonnes).

Initial population

The initial population was made up of the 12 vessels in Table 2 and Figures 36A/B and 37A/B.

In both Case Studies 4 and 5, the heading angle was set at 45 degrees (where head sea = 0 degree) for seakeeping calculation. Two-point cross-morph was applied to increase the variety of solutions in both case studies as multi-objective optimisation problems tended to stagnate quickly. In this method, blending is conducted using two crossover points between

three vessels, instead of one crossover point between two vessels, as in a single point crossover. This approach allows a larger variety of vessels to be combined and therefore ensures that more varied shapes are created. This is achieved by altering the chromosomes of the three different parent vessels and their connections (transition frames). Figure 57 provides the resultant hull obtained following two-point cross-morph of three different parent vessels. Here, the forward section of ship 9 (VLCC), the mid-body of ship 1 (container A) and aft-body of ship 7 (product tanker) were used. Two transition sections that connected the existing vessel bodies were produced using two-point cross-morph with the intersection (crossover) points indicated by the full shaded planes. From the encoding (mapping) scheme shown, it may be observed that the cross-morph enables a smooth transition by varying the morphing parameters between the three different parent vessels. This example demonstrated the ability of two-point cross-morph to 'cut-and-joint' multiple hull sections into one seamless hull form which helped to create more shape variations.

Case Study 4: Two-Objective Functions (Resistance and Heave)

The goal in Case Study 4 was to minimise the resistance and heave of the vessel, both of which are non-conflicting objectives. The settings used were as follows:

- Initial population = 12 vessels
- Crossover rate = 0.5 to 1.0
- Mutation rate = 0.5 to 1.0
- Number of generations = 100

Similar to the previous case studies, 36 simulations were performed with different combinations of crossover and mutation rates in the range of 0.5 to 1.0. Figures 58 and 59 shows the convergence charts of total resistance and heave respectively. The results show the resistance tended to stagnate for lower crossover and mutation rates (< 0.6). This could have limited shape variations and hence the number of good solutions that can be carried over to the next generation is reduced. Heave performance continued to improve as the crossover and mutation rates increase. It was also observed that when the mutation rate increased to 0.9 and 1.0, the search converged prematurely. This was likely because a high mutation rate could have 'over-manipulated' the structures, and destroyed good features from reproduction and crossover. Therefore, a balance between crossover and mutation rates is crucial to the success of optimisation. For ease of comparison, the best individual for each crossover-mutation rate combination is shown in Table 12. The best result for each of the overall best resistance and heave for the respective crossover and mutation rates

are indicated in the table. It should be noted that no individual solution is best for both objectives.

Table 12: Best results at final generation for total resistance and heave for each crossover and mutation rates.

Crossover rate	Mutation rate	Total resistance (kN)	Heave
0.5	0.5	266.4	1.76
	0.6	268.4	**1.62 (best)**
	0.7	311.3	1.76
	0.8	290.4	1.70
	0.9	257.8	1.75
	1.0	**255.3 (best)**	1.69
0.6	0.5	270.3	1.63
	0.6	264.8	1.63
	0.7	289.1	**1.61 (best)**
	0.8	273.4	1.62
	0.9	**255.2 (best overall)**	1.65
	1.0	268.7	1.73
0.7	0.5	**259.3 (best)**	1.78
	0.6	265.8	1.71
	0.7	276.7	1.63
	0.8	273.5	**1.58 (best overall)**
	0.9	259.4	1.72
	1.0	269.1	1.59
0.8	0.5	259.9	1.70
	0.6	272.2	**1.59 (best)**
	0.7	268.8	1.71
	0.8	264.3	1.64
	0.9	263.5	1.71
	1.0	**259.1 (best)**	1.74
0.9	0.5	262.2	1.76
	0.6	261.3	1.79
	0.7	280.3	**1.66 (best)**
	0.8	266.3	1.76
	0.9	264.4	1.67
	1.0	**256.1 (best)**	1.76
1.0	0.5	270.7	1.77
	0.6	262.6	**1.65 (best)**
	0.7	262.5	1.72
	0.8	267.7	1.84
	0.9	272.7	1.81
	1.0	**258.2 (best)**	1.77

The best resistance was obtained when the crossover rate was 0.6 and the mutation rate was 0.9. It was observed that a lower crossover rate appeared to have a better effect on resistance performance. Considering that a two-point crossover is used in this case, a high crossover rate may be too disruptive, resulting in the vessel shape becoming overly irregular. This has a direct impact on the hydrodynamic (flow) performance. Mutation, on the other hand, only introduces subtle changes to the hull. The best heave was obtained when the crossover rate was 0.7 and the mutation rate was 0.8. In this case, a slightly higher crossover rate may have helped to create more varied form factors, which had positive impacts on seakeeping performances. Conversely, it was also found that too high a crossover rate might have resulted in over-varied form factors or irregular shapes, hence worsened seakeeping performance.

For further investigation, the solution for crossover at 0.6 and mutation at 0.9 was selected due to it having suitable results for both objective functions. The combined convergence chart and solution space for resistance and heave is shown in Figures 60 and 61 respectively. From Figure 60, it may be observed that the resistance value increased at the start and came down gradually after 10 generations. This could be due to the trade-off of one objective (resistance) for the improvement of the other objective (heave). Subsequently, both objectives stabilised at the lowest value after the 30th generation. This demonstrated the ability of MEC to find an optimal solution even with more than one objective.

In Figure 61, the solutions may be grouped into three regions which illustrate how the design space was explored by the MEC methods. Region 1 shows the solutions found in the first 40 generations and are well spread across the design space for both objectives. This suggests that the selection and reproduction mechanisms were able to find preliminary designs that are further refined as the optimisation progressed. This was evident by observing the solutions in region 2 which have better resistance than those in region 1. Finally, in region 3, the optimisation converged to a set of Pareto optimal solutions satisfying both objectives for resistance and heave motions.

To ascertain the efficacy of MEC, three comparisons were conducted. First, the best solutions obtained from the optimisation were compared to the cable-laying vessel (Ship 11) in the initial population in terms of their cable-laying performance. The latter was manually optimised by a designer. Second, for each objective, each of the best solutions was benchmarked against the best performing parent solution for that objective. For

example, the resistance of all the best solutions found at the end of the optimisation was compared against that of the parent vessel (ship 1 – container Ship A) which has the best resistance amongst all parent solutions in the initial population. Third, the quality of the solutions obtained from MEC was compared against one another. This provided insights into their feasibility as well as the choice of the solutions available to the designer at the end of the optimisation. The performance of the best initial parents and best solutions are presented in Table 13 and the percentage difference between the parent and child is shown.

Table 13: Best parent and child solutions

Best parent / Best Child	Best heave – Ship 11 (Cable-laying Ship) Resistance = 352.04 kN Heave = 2.02		Best resistance - Ship 1 (Container Ship A) Resistance = 278.54 kN Heave = 2.65		
Solution	**Resistance**	**Heave**	**Resistance**	**Heave**	**Displacement, tonnes**
	(% improvement over best parent)				
1189	263.42 (25.17)	2.01 (0.44)	263.42 (5.42)	2.01 (21.11)	15062.23
1190	283.38 (19.50)	1.65 (18.17)	283.38 (-1.73)	1.65 (37.62)	15018.99
1191	283.38 (19.50)	1.65 (18.17)	283.38 (-1.73)	1.65 (37.62)	15018.99
1192	256.7 (27.07)	2.70 (-34.09)	256.7 (7.83)	2.70 (-2.21)	15101.53
1193	262.06 (25.55)	2.55 (-26.27)	262.06 (5.91)	2.55 (3.74)	15000.01
1194	255.25 (27.49)	2.81 (-39.22)	255.25 (8.35)	2.81 (-6.12)	15019.29
1195	288.20 (18.13)	1.67 (17.03)	288.20 (-3.47)	1.67 (36.75)	15257.98
1196	271.72 (22.81)	1.89 (5.96)	271.72 (2.44)	1.89 (28.32)	15042.73
1197	269.21 (23.52)	1.96 (2.74)	269.21 (3.34)	1.96 (25.86)	15123.11
1198	264.55 (24.85)	2.46 (-22.00)	264.55 (5.02)	2.46 (6.99)	15067.05
1199	273.09 (22.42)	1.87 (7.13)	273.09 (1.95)	1.87 (29.21)	15260.39
1200	271.87 (22.77)	2.40 (-19.27)	271.87 (2.39)	2.40 (9.08)	15066.43

There are several key observations from Table 13. All the 12 near-optimal solutions outperformed the best initial parent (ship 11) in terms of resistance (mean improvement, μ = 23.23%). Of these solutions, seven child solutions showed an average improvement of 9.95% in heave. In comparison to ship 1 (Container Ship A) which was the best parent vessel in terms of resistance, nine of the child solutions showed an average improvement of 4.74% in resistance and 10 child solutions showed an average improvement of 23.93% in heave. By comparing all the child solutions, solutions 1189, 1196, 1197, 1199 may be considered optimal solutions, which demonstrated improvement over both best initial parent ship 1 and ship 11.

To better understand the results from a naval architect's perspective, the hull forms of the best child solutions for heave (solution 1190) and resistance (solution 1194) are shown in Figure 62. The cross-sectional areas of solution 1190 in Figure 62(a) were substantially equal across the entire length of the vessel, which helped in reducing the heave motion. In Figure 62(b), the forward and aft body of solution 1194 had much smaller cross-sectional areas when compared to the mid-body. As a result, the vessel had a narrower forward and aft section and therefore a lower resistance.

Figure 63 shows the body plans for the best initial parents and best child solutions comprising of (a) best child (solution 1190) and best parent (Ship 11) with lowest heave and (b) best child (solution 1194) and best parent (Ship 1) with lowest resistance. It may be seen that there is some resemblance in the shapes of both best child solutions to the initial parent vessels. In Figure 63(a), the extreme bow and aft section of solution 1190 are very similar to ship 11 (Cable-laying Ship). However, the mid-section looks rather different. This is because during the two-point cross-morph the child solution was created by merging ship 3's (Container Ship C) mid-body and ship 11's forward and aft body from the initial population. In Figure 63(b), the forward section of solution 1194 is similar to ship 1 (container ship A). It was observed that the mid and stern sections were created by merging ship 8 (Chemical Tanker) and ship 6 (Bulk Carrier) using cross-morph. In both cases, the vessels were further modified with boundary-morph during mutation.

The total time taken for each optimisation was approximately 16 hours, using a 4-core CPU. 36 simulations were completed to compare results from varying crossover and mutation settings. As compared to the single-objective optimisation presented above, the duration

has increased significantly due to the additional seakeeping performance evaluation using strip theory.

Case Study 5: Multi-Objectives Function (Resistance, Heave, Roll and Pitch)

In case study 5, two more objectives, roll and pitch were added to resistance and heave to demonstrate the performance of MEC for multi-objective optimisation involving both non-conflicting and conflicting objective functions. The same parent vessels in Case Study 4 were used as starting points. The following settings were used:

- Initial population = 12 vessels
- Crossover rate = 0.5 to 1.0
- Mutation rate = 0.5 to 1.0
- Number of generations = 100

36 simulations were performed using different combinations of crossover and mutation rates, between 0.5 and 1.0. The convergence charts of total resistance, heave, pitch and roll are shown in Figures 64 to 67 respectively.

For comparison of the four objective functions (total resistance, heave, pitch and roll), the best results at the final generation for each crossover-mutation rate combination are presented in Table 14. As these involve conflicting objectives, no individual solution had the best performance in all four objectives, the best result for each crossover rate and the overall best result for each objective are indicated.

Several observations were made from Table 14. The best performance for each objective generally worsened (increased) as the crossover rate increased, except for pitch which remained approximately constant. For example, the best performance for resistance increased from 245.5 kN at a crossover rate of 0.5 to 260.5 kN at a crossover rate of 1.0. The best performance for heave increased from 1.62 to 1.64, at crossover rates of 0.5 and 1.0, respectively. This was the same for roll, which increased from 0.08 at a crossover rate of 0.5, to 0.11 at a crossover rate of 1.0. This trend was consistent with multi-objective case study 4, where higher crossover rate tended to cause too many shape changes during cross-morph, resulting in poorer performances.

Table 14: Best results for total resistance, heave, pitch and roll for different combination crossover and mutation rates from 0.5 to 1.0.

Crossover rate	Mutation rate	Total resistance	Heave	Pitch	Roll

0.5	0.5	245.5 (best for total resistance)	1.74	0.56 (best pitch for crossover rate)	0.13
	0.6	250.0	1.88	0.56	0.08 (best roll for crossover rate)
	0.7	257.5	1.73	0.57	0.17
	0.8	257.5	1.67	0.56	0.09
	0.9	263.9	1.71	0.67	0.13
	1.0	261.7	1.62 (best for heave)	1.15	0.17
0.6	0.5	245.7 (best total resistance for crossover rate)	1.72	0.58	0.14
	0.6	258.0	1.75	0.56 (best pitch for crossover rate)	0.10
	0.7	254.1	1.76	0.59	0.19
	0.8	255.9	1.68 (best heave for crossover rate)	0.58	0.13
	0.9	266.4	1.82	0.56 (best pitch for crossover rate)	0.08 (best roll for crossover rate)
	1.0	249.8	1.69	0.98	0.20
0.7	0.5	265.4	1.86	0.59	0.17
	0.6	270.5	1.79	0.56 (best pitch for crossover rate)	0.11
	0.7	261.4	1.67 (best heave for crossover rate)	0.59	0.16
	0.8	264.2	1.76	0.60	0.17
	0.9	257.8 (best total resistance for crossover rate)	1.74	0.60	0.12
	1.0	259.2	1.67 (best heave for crossover rate)	0.93	0.07 (best for roll)
0.8	0.5	255.3 (best total resistance for crossover rate)	1.73	0.81	0.16

	0.6	264.0	1.86	0.55 (best for pitch)	0.12
	0.7	261.2	1.85	0.62	0.08 (best roll for crossover rate)
	0.8	270.5	1.77	0.59	0.33
	0.9	256.0	1.71 (best heave for crossover rate)	0.58	0.10
	1.0	286.0	1.72	1.17	0.11
0.9	0.5	261.2	1.81	0.56	0.08 (best roll for crossover rate)
	0.6	267.7	1.74	0.59	0.15
	0.7	256.8 (best total resistance for crossover rate)	1.85	0.58 (best pitch for crossover rate)	0.16
	0.8	257.8	1.73 (best heave for crossover rate)	0.60	0.19
	0.9	262.5	1.75	0.63	0.10
	1.0	268.7	1.74	0.98	0.11
1.0	0.5	280.0	1.83	0.60	0.13
	0.6	270.6	1.80	0.61	0.19
	0.7	260.4 (best total resistance for crossover rate)	1.75	0.56 (best pitch for crossover rate)	0.13
	0.8	275.3	1.81	0.59	0.11 (best roll for crossover rate)
	0.9	265.8	1.76	0.59	0.15
	1.0	278.3	1.64 (best heave for crossover rate)	1.19	0.20

Furthermore, by comparing the different mutation rates for each objective, better performances were observed when a higher mutation rate was used to balance a lower crossover rate. For example, better performances for pitch and roll were achieved at a crossover rate of 0.6 and a mutation rate of 0.9, and better performance for heave and roll were achieved at a crossover rate of 0.7 and a mutation rate of 1.0. Overall, this trend was

consistent with the two-objective case study 4, where higher mutation rates were required to further refine the shape through subtle changes using boundary-morph.

However, where a high crossover rate was used, such as 0.8 or 0.9, too many shape changes may occur and result in a poorer performance. Based on these findings, the crossover and mutation rates with the best (lowest) resistance were found to be 0.5 and 0.5, the best (lowest) heave was 0.5 and 1.0, the best pitch was 0.8 and 0.6 and the best roll was 0.7 and 1.0, respectively. For further investigations, the best solution for crossover at 0.7 and mutation at 1.0 was selected as they generated better results for the most objective functions.

By comparing the results obtained for each objective function, it may be seen that the best results were obtained for both resistance and pitch in several settings (e.g. crossover 0.5 and mutation 0.5, crossover 0.9 and mutation 0.7), which demonstrated they were non-conflicting. However, it may also be seen that both resistance and pitch worsened (increased) when heave or roll objective function was at its peak (lowest). This shows that both resistance and pitch were conflicting to heave and roll function respectively.

The combined convergence chart for resistance, heave, pitch and roll is presented in Figure 68. It may be seen from the combined convergence chart that all the objectives improved (reduced) concurrently and reached the minimum after the 20th generation. Similar to the two-objective case study 4, the fitness for pitch and roll were increased at the initial point due to performance trade-offs, but subsequently decreased when it began to balance and reach its near-optimal point.

As four objectives were considered in this optimisation, a total of six pairs of objective comparisons is shown in Figures 69-74. Initial observations on the overall distribution of the solutions for each objective pair showed that the solutions were dispersed across the design space. By examining the distributed solutions in generations 91–100, two main trends were observed. Firstly, from Figures 69 and 70, most of the solutions converged towards the bottom-left hand corner as the optimisation progressed. In particular, from Figures 71 and 72, a clear Pareto front emerged at the final generations. This demonstrated the ability of MEC to produce near-optimal solutions.

Figures 73 and 74 showed that the solutions generally converged towards the better performance of only one objective indicating that most of the best solutions may only satisfy one design objective but not the other. A possible interpretation may be that while a larger Pareto optimal solution set is not uncommon for a higher number of objectives, it becomes more challenging to find solutions that meet all design criteria as the number of design criteria increases.

This phenomenon may be observed by comparing the convergence plots in Figure 69 and Figure 61 (case study 4) for resistance vs heave where the latter had only two objectives to optimise. The performance in case study 5 was more levelled such that it may perform slightly worse in one objective and better in another to achieve a more balanced solution.

The performance of the best parent and child solutions obtained at the end of the optimisation is shown in the table in Figure 75. The values in the brackets shows the percentage difference between the solution and the best parent for a particular objective. A positive value indicates an improvement over the parent, while a negative value indicates a worse performance compared to the parent. The values for the best solution for each objective is provided in bold and italics.

Three performance comparisons were done for Case Study 5 where the group of Pareto optimal solutions were first compared with the cable-laying vessel in the initial population. Comparisons were then conducted at the objective level where the pool of optimal solutions were benchmarked against the best performing parent vessel for each objective and finally the performance of each Pareto optimal solution in the Pareto was compared with one another.

From Figure 75, three Pareto optimal solutions (1190, 1198, 1120) had at least three objective functions that were superior to ship 11. Among these, solution 1190 exceeded the performance of an existing cable-laying vessel, which was manually optimised by the designer, for all objective functions. This demonstrated that the methods described herein allows all design criteria to be met, including outperforming existing proven designs. On the whole, each child solution had at least two objectives that were superior to the parent solution.

Taking each objective in turn, the performance between a child solution and the best parent solution were also compared. From Figure 75, a large number of solutions outperformed the best parent for each objective. For example, solutions 1190, 1198, 1120 for heave, solution 1192 for resistance, solutions 1191, 1195, 1196, 1197, 1198, 1199, 1120 for pitch and solution 1193 for roll. More notably, most child solutions had better performances where three of the four objective functions were satisfied, when compared to the best parent solutions. The methods described allows the hull form design optimisation process to be performed more efficiently and achieve similar if not better quality compared to existing processes by a designer. In addition, more solutions may be explored without bias from the designer.

When the Pareto optimal solutions were compared to one another, the best solution for heave was solution 1190 (1.67), the best solution for resistance was solution 1192 (259.26 kN), the best solution for pitch was 1191 (0.93) and the best solution for roll was 1193 (0.07). When compared to the best solution (1190), solution 1192 had two objectives that were better (resistance and roll) and solutions 1191 and 1193 had one objective (pitch and roll respectively) that were better than solution 1190. The wire-mesh diagrams and body plans of the best child solutions for the objective functions are presented in Figures 76 and 77 respectively.

From Figure 76, it may be observed that each best child solution had a different hull form for each objective. For example, solution 1190 in Figure 76(a) showed a fuller hull form that was relatively uniform across the length of vessel, which resulted in lower heave. The hull form of solution 1192 in Figure 76(b) was sharp at the bow and had a slender body which was good for resistance. Figure 76(c) showed that solution 1191 had a hull form with a full bow and wide aft section which provided lower pitch. Figure 76(d) showed that solution 1193 had a hull form that was relatively full at the mid-body and slender at the aft, which helped to reduce the roll motion. All the hull forms in Figure 76 were highly feasible without abrupt shape changes or unevenness. It was observed that solutions 1192 and 1193 may not be suitable for an offshore cable-laying vessel due to the small transom that limits cable-laying operations (this not being an objective in the method).

Figure 77 showed that the best child vessels (dotted line) had very different hull forms from their best parent vessels (solid line), although there were some resemblance at different

parts of the body section. For example, it may be seen from Figure 77(a) that both the forward and aft section of best child solution 1190 (heave) was inherited from parent ship 11, a cable-laying vessel. This highlights the fact that MEC was able to search the design space to find existing solutions which were close to the design specification and at the same time create new vessels through crossover and mutation. Solution 1192 (resistance) is a combination of ship 4, 6 and 10 as seen in Figure 77(b). The aft section took the shape of ship 4 (Container Ship D), while the mid-section resembled that of ship 6 (Bulk Carrier) and the forward section took its shape from ship 10 (Pipe-laying Ship).

For best child solution 1191 (pitch) in Figure 77(c), the aft section takes the shape of the best parent: ship 11 (Cable-laying Ship), the mid-section resembles ship 6 (Bulk Carrier) and the forward section from ship 10 (Pipe-laying Ship). Finally, best child solution 1193 shown in Figure 77(d) inherited properties from parent ships 4, 8 and 11. For example, the aft section resembles ship 4 (Container Ship D), the mid-section resembles ship 8 (Chemical Tanker) and the forward section takes the shape of ship 11 (Cable-laying Ship). The time taken for each optimisation case was approximately 16 hours on a 4-core CPU. In total, 36 simulations were completed using parallel computing, which reduced the processing time to under five days.

Optimisation using Goal-setting Approach

From the four-objective Case Study 5, some of the solutions found in the final generation (in particular Figures 73 and 74) had extremities where an individual objective tends to dominate. Although these solutions are near-optimal, in practice they may not be useful to the designer as they may not be considered all-rounded solutions that satisfy both the objective functions. To avoid this the solution space may be narrowed down by applying the goal-setting approach. This was performed by constraining the search space such that any individuals created that do not meet the constraints set were eliminated and were not carried over to the next generation.

To set the constraints and thereby the boundaries of the search space, the best performing parent in the initial population for each objective were used as benchmarks. The constraints were set at +/- 5% of the best objective values. The additional constraints for each objective function were provided in Table 15.

Table 15: Upper and lower limit constraints set for each objective function.

Objective functions	**Lower limit (minimum) constraint**	**Upper limit (maximum) constraint**
Resistance	278.54 kN (ship 1) × 95% = 264.61 kN	503.19 kN (ship 10) × 105% = 528.34 kN
Heave	2.02 (ship 11) × 95% = 1.91	3.21 (ship 4) × 105% = 3.37
Pitch	1.3 (ship 10) × 95% = 1.23	5.75 (ship 4) × 105% = 6.03
Roll	0.22 (ship 7) × 95% = 0.2	32.53 (ship 1) × 105% = 34.15

The optimisation was performed using the best crossover and mutation rates of 0.7 and 1.0 obtained from Case Study 5, and the results were presented in Figure 78. It may be observed that the individual solutions were generally scattered within the constraint limits, except in Figure 78(e), where extremities were still found on either side of the objective functions. This could be attributed to the conflicting nature of the heave and roll motion, where the improvement of one function result in worsening of the performance of the other. By comparing the goal-setting and non-goal-setting case in Case Study 5, it may be seen from Figure 78 that the individuals were generally more spread out compared to Figures 69-74. In particular, the solutions found in the final population were more scattered around the solution space, whereas in Figures 69-74 the solutions converge towards the bottom-left hand corner. The best individuals for each objective were compared in Table 16.

Table 16: Comparison of best results obtained for each objective with and without goal-setting

	Best parent from initial population	**Best child (without goal-setting)**	**Improvement over best parent**	**Best child (with goal-setting)**	**Improvement over best parent**
Resistance (kN)	278.54	259.2	6.94%	264.61	5.13%
Heave	2.02	1.67	17.32%	1.91	5.94%
Pitch	1.3	0.93	28.46%	1.4	-7.69%
Roll	0.22	0.07	68.18%	0.22	0%

From the results in Figure 78 and Table 16, goal-setting provided greater diversity in the solutions found, as they were more spread out. However, the overall performance was not improved. When the solutions obtained using goal-setting were compared to the best parent in the initial population, i.e. designs produced by experienced designers, only 50% of the objectives showed better performance. On the other hand, when no goal-setting was applied, the solutions found outperformed the best parent vessel for all four objectives.

Comparing the best child with and without goal-setting, it appears the latter was inferior. The reason for this result may be due to the small constraints (+/- 5%), which led to a relatively small impact on the performance. Another possible reason may be due to the small population size where it cannot afford to eliminate any potentially good individual which could be carried forward to the future generation.

Several observations may be made from case studies 4 and 5. Most of the child solutions achieved better performance over the parent solutions in all objective functions in case study 4 while solutions in case study 5 typically achieve good improvements for up to three out of four objectives. By comparing the performance improvement over best initial parents in case study 4, solution 1190 achieved 18.17% improvement in heave over best parent (ship 11) while solution 1194 achieved 8.35% improvement in resistance over best parent (ship 1). In case study 5, solution 1190 achieved 17.43% improvement in heave over best parent (ship 11), solution 1192 achieved 6.93% improvement in resistance over best parent (ship 1), solution 1191 achieved 28.45% improvement in pitch over best parent (ship 10) and solution 1193 achieved 66.75% improvement in roll over best parent (ship 7).

Further, it was clear from both case studies that the results produced by MEC for the multi-objective optimisations were better with crossovers between 0.6 and 0.7 and mutation rates between 0.9 and 1.0. In the case of the two-objective optimisation, it was found that crossover at 0.6 and mutation at 0.9 provided the best results. In the four-objective optimisation problem, crossover at 0.7 and mutation at 1.0 were found to provide the best results. It was observed that high crossover settings may cause “over-variation” of the hull shape, which may be too disruptive to the shape of the hull and led to negative results. High mutation, on the other hand, provided subtle variations or shape refinements through boundary-morph, while keeping the main body of the vessel following crossover intact, leading to better performances.

Further, from the table in Figure 75 most solutions did not exhibit good roll and resistance. In fact, only one of the 12 child solutions had better resistance performance and one child solution had better roll motion when compared to the best parent solution for these objectives. When ranked according to the number of solutions which performed better than the best parent vessel, it was shown that roll and resistance was the hardest objective function to optimise, followed by heave and pitch.

Further, it was observed that where two optimisation problems have overlapping objective functions, the one with a larger set of objectives tended to perform worse than the problem with a smaller set of objectives when the same objective functions were compared. This may be because a Pareto optimal solution in the larger set had more objectives to “balance” in order to find a more all-rounded solution.

Existing processes for conflicting multi-objective optimisation processes are very tedious, using conventional trial and error methods as improving one objective function would very likely result in worsening the performance of others. The methods described herein allows the manual search process to be done more efficiently and without bias from a human designer.

Case study 5 also showed that the methods described could “mimic” the human designer by automatically deciding which objectives to “sacrifice” while improving others to achieve more balanced solutions. This is beneficial as it offers the designer a pool of feasible solutions to further work on if necessary. A near-Pareto optimal solution (1190) exceeded the performance of an existing cable-laying vessel, for all the set objective functions, thus proving the feasibility of the methods described to allow for a new hull design to be achieved without requiring human input beyond the initial parameters.

Furthermore, by maintaining a small population of individuals throughout the optimisation, the methods described provides a methodical way to derive the solutions. This allows the designer to trace the key steps of how a child solution was generated in a constructive manner and gained better insights into the design and may help towards alleviating the ‘designer’s dilemma’ in selecting the best design to a multi-objective optimisation problem.

A more ‘balanced’ solution may be achieved when optimising more than two objective functions. In consideration, MEC may be applied effectively for optimising many objective optimisations involving conflicting and non-conflicting seakeeping functions, and to create many possible new design combinations and automatically narrow to a few good solutions. This may serve as a useful tool to guide the designer on which design to develop further.

MEC allows for a fully automated hull form design and optimisation tool that requires minimal user input. Conventional SBD tools require expert input to set the direction for automated simulation, and may be limited by the experience and bias of the designer. MEC allows the design optimisation to start from proven body designs, the exploration of wider solution spaces and creation of more optimal hull forms. The MEC may shorten the entire design process while evaluating more possibilities.

Some existing methods require additional pre-check steps such as design-of-experiment to ensure that variations defined by the designer helps to reasonably improve the design with no unfeasible designs and to investigate the influence of parameters on the objectives and to provide a preliminary idea of the expected performance and parameters which have the most impact on the overall design optimisation process. MEC eliminates the need for this pre-qualification check since all base-line designs used from the hull form library are feasible. By performing morphing via interpolation and extrapolation between these proven designs, it enables automated geometry modification with minimal designer input.

The phenotype-genotype mapping developed provides an elegant and effective way to transform the hull form into an optimisation problem. Hull lines are simple to represent in phenotype spaces within GA and provide more flexibility for shape modification compared to surfaces. Through unique crossover and mutation functions, the entire hull shape may be ‘mix-and-match’ and transformed using the morphing parameter t, which enables the creation of more innovative hull forms. This approach has the flexibility of combining two or more different hull forms together, thereby increasing the solution space for more optimal hulls. It should be noted that the MEC approach is not limited to only ship hull forms and may similarly be applied to other vehicles that require a streamlined profile be it on land, sea or air. For example, the methods described herein may be extended to other geometry-related design applications such as airplanes and automobile main body design by using different fitness evaluation methods. A difference between these different vehicle designs is the density of the medium and speed, and possibly how the geometry may be

represented, which may not always be in the form of an offset table. Nonetheless, their geometries may still be mapped into 2D space and be applied into the MEC method.

The systems and methods described above may be implemented in many different ways in many different combinations of hardware, software, firmware, or any combination thereof. In one example, the systems and methods may be implemented with a computer having a processor and a memory communicably coupled thereto, where the memory stores instructions which when executed by the processor, cause the processor to perform the aforementioned methods. The processor may include any type of circuit such as, but not limited to, a microprocessor, a microcontroller, a graphics processor, a digital signal processor, or another processor. The processor may also be implemented with discrete logic or components, or a combination of other types of analogue or digital circuitry, combined on a single integrated circuit or distributed among multiple integrated circuits. All or part of the logic described above may be implemented as instructions for execution by the processor, controller, or other processing device and may be stored in a tangible or non-transitory machine-readable or computer-readable medium such as flash memory, random access memory (RAM) or read only memory (ROM), erasable programmable read only memory (EPROM) or other machine-readable medium such as a compact disc read only memory (CDROM), or magnetic or optical disk. A product, such as a computer program product, may include a storage medium and computer readable instructions stored on the medium, which when executed in an endpoint, computer system, or other device, cause the device to perform operations according to any of the description above. The memory can be implemented with one or more hard drives, and/or one or more drives that handle removable media, such as diskettes, compact disks (CDs), digital video disks (DVDs), flash memory keys, and other removable media.

The new body design/s, in particular hull designs, may be used in a method to build a vehicle, e.g. a marine vessel, in particular a ship, by manufacturing the vehicle based on the body design/s or the new set of body designs.

Whilst there has been described in the foregoing description preferred embodiments of the invention, it will be understood by those skilled in the field concerned that many variations or modifications in details of design or construction may be made without departing from the present invention.

Claims

1. A computer implemented method of generating a new body design for a new vehicle, the method comprises:
   (a) providing an initial body design of a vehicle in a two-dimensional space with a plurality of frame lines;
   (b) selecting a first boundary frame line of the initial body design and a second boundary frame line of the initial body design;
   (c) selecting a first reference frame line between the first boundary frame line and the second boundary frame line;
   (d) selecting a morphing parameter, wherein the morphing parameter is a rate of change between the first reference frame line and the first boundary frame line and/or the second boundary frame line;
   (e) modifying the initial body design from the first reference frame line towards the first boundary frame line and/or from the first reference frame line towards the second boundary frame line based on the morphing parameter; and
   (f) generating the new body design.

2. The method according to claim 1 wherein there is at least one intermediate frame line between the first reference frame line and the first boundary frame line and/or the first reference frame line and the second boundary frame line, and the method further comprises adjusting the at least one intermediate frame line based on a modified morphing parameter.

3. The method according to any one of claims 1 to 2 further comprises selecting a third boundary frame line of the initial body design; selecting a second reference frame line between the second boundary frame line and the third boundary frame line; selecting a second morphing parameter, wherein the second morphing parameter is a rate of change between the second reference frame line and the second boundary frame line and/or the third boundary frame line and modifying the initial body design from the second reference frame line towards the second boundary frame line and/or towards the third boundary frame line based on the second morphing parameter.

4. The method according to any one of claims 1 to 3 wherein the first, second, and/or third boundary frame lines is a non-terminal frame line.

5. The method according to any one of claims 1 to 4, wherein the first boundary frame line is selected proximal to a first end of the initial body design and the second boundary frame line is selected proximal to a second end of the initial body design, the second end being opposite to the first end.

6. The method according to claim 5, wherein the first end is a forward section of the initial body design, the second end is an aft section of the body design, and the third boundary frame is selected proximal to the middle of the initial body design.

7. The method according to any one of claims 1 to 6, wherein the morphing parameter is randomly selected.

8. The method according to any one of claims 1 to 7, wherein the first reference frame line and/or the second reference random frame line is/are randomly selected.

9. The method according to any one of claims 1 to 8, wherein modifying the initial body design is based on the following:

$Y(t = x_R \times W)_{R_{x,z}} = (1 - (t \times S_{TS})) \times Y_{S_{x,z}} + (t \times S_{TS}) \times Y_{T_{x,z}}$,

where $W = 0.02 \times (x - x_{AB})$ when $x_{AB} \leq x \leq x_{MB}$ and $W = 0.02 \times (x - x_{MB})$ when $x_{MB} \leq x \leq x_{FB}$;

$Y(t = x_A \times \omega)_{A_{x,z}} = (1 - (t \times S_{TS})) \times Y_{S_{x,z}} + (t \times S_{TS}) \times Y_{T_{x,z}}$,

where $W = 0.04 \times (x - x_R)$ when $x_R \leq x \leq x_{MB}$ and $x_R \leq x \leq x_{FB}$,

$W = 0.04 \times (x_R - x)$ when $x_{AB} \leq x \leq x_R$, and

$W = 0.04 \times (x - x_{MB})$ when $x_{MB} \leq x \leq x_R$;

subject to $0.2 \leq t \leq 0.8$ and smoothing factor, $S_{TS} = 1 - \frac{Y_{TS}}{B_{max}}$,

where $Y(t)_{R_{x,z}}$ is the new *Y* value for the reference curve at corresponding *x* and *z* coordinates, $Y(t)_{A_{x,z}}$ is the new *Y* value for adjacent curves at corresponding *x* and *z* coordinates, $Y_{S_{x,z}}$ is the *Y* value for the reference (source) curve at corresponding *x* and *z* coordinates and $Y_{T_{x,z}}$ is the *Y* value for the boundary (target) curve at corresponding *x* and *z* coordinates. x_A is the x coordinate of the adjacent frame between the reference frame and boundary frames, $x_{F/AB}$ is x frame at the forward or aft boundary section, x_R is x frame at the reference frame section and x_{MB} is x frame

at the mid boundary section. W is the weightage, Y_{TS} is the Y value of the transition section between the two boundaries and B_{max} is the maximum ½ breadth.

10. The method according to any one of claims 1 to 9, wherein the vehicle is a ship.

11. The method according to any one of claims 1 to 10, wherein providing the initial body design in a two-dimensional space with a plurality of frame lines comprises providing dimensions of the initial body design in a two dimensional offset table and mapping the dimensions in the two dimensional offset table into a two dimensional line plan to obtain the plurality of frame lines.

12. A computer implemented method of generating a new set of body designs for a new vehicle, the method comprises:
    (a) providing a set of body designs of a vehicle;
    (b) evaluating each body design in the set with respect to at least one objective function;
    (c) performing a crossover combination of a plurality of body designs from the set to provide a plurality of initial body designs based on a crossover rate, wherein the crossover rate is a probability of the combination occurring;
    (d) providing each of the plurality of initial body designs in a two-dimensional space with a plurality of frame lines;
    (e) selecting a first boundary frame line of each of the initial body designs and a second boundary frame line of each of the initial body designs;
    (f) selecting a first reference frame line between the first boundary frame line and the second boundary frame line;
    (g) selecting a morphing parameter, wherein the morphing parameter is a rate of change between the first reference frame line and the first boundary frame line and/or the second boundary frame line;
    (h) modifying each of the initial body designs from the first reference frame line towards the first boundary frame line and/or from the first reference frame line towards the second boundary frame line based on the morphing parameter and a mutation rate, wherein the mutation rate is a probability of applying the morphing parameter to modify the initial body design;
    (i) generating a plurality of new body designs;
    (j) evaluating the plurality of new body designs based on the at least one objection function;

(k) ranking the body designs in the set of body designs and in the plurality of new body designs based on the evaluation of the at least one objective function; and

(l) generating a new set of body designs based on the ranking.

13. The method according to claim 12 further comprises selecting the plurality of body designs randomly from the set of body designs to perform the crossover combination or selecting the plurality of body designs based on the evaluating step to perform the crossover combination.

14. The method according to claim 13, further comprises rescaling at least one of the body designs in the selected plurality of body designs prior to performing the crossover combination.

15. The method according to any one of claims 12 to 14, wherein ranking the body designs comprises sorting the body designs in the set of body designs and the plurality of new body designs to determine at least one Pareto front; measuring a distance between each body design in each of the at least one Pareto front; and ordering the body designs in the set of body designs and the plurality of new body designs based on the at least one Pareto front and the distance between the body designs in each Pareto front.

16. The method according to any one of claims 12 to 15 further comprises repeating steps (c) to (l) using the new set of body designs until convergence of the body designs or a maximum number of iterations is reached.

17. The method according to any one of claims 12 to 16, wherein the at least one objective function is any one selected from the group consisting of manoeuvrability, resistance, seakeeping, stability, and structural strength.

18. The method according to any one of claims 12 to 17, wherein the set of body designs comprises a plurality of existing body designs.

19. The method according to claim 18, wherein the set of body designs comprises at least one modified body design obtained by interpolating and/or extrapolating a first existing body design and a second existing body design.

20. The method according to claim 19, wherein each of the first existing body design and the second existing body design is represented in a two dimensional plane at a plurality of locations along a third dimension perpendicular to the two dimensional plane.

21. The method according to any one of claims 12 to 20, wherein the crossover rate and/or mutation rate is at least 0.5.

22. The method according to claim 21, wherein the crossover rate and/or mutation rate is at least 0.7.

23. The method according to any one of claims 12 to 22, wherein the new set of body designs has the same number of body designs as the set of body designs.

24. A method to build a vehicle, the method comprises obtaining the new body design for a vehicle according to any one of claims 1 to 11 or obtaining the new set of body designs for a vehicle according to any one of claims 12 to 23, and manufacturing the vehicle based on the new body design or the new set of body designs.

25. A non-transitory computer readable medium comprising instructions which, when executed by a computer, cause the computer to perform a method according to any one of claims 1 to 23.